



U.S. Department of
Transportation

**Federal Railroad
Administration**

Locomotive Fuel Tank Structural Safety Testing Program: Passenger Locomotive Fuel Tank Jackknife Derailment Load Test

Office of Research
and Development
Washington, DC 20590



NOTICE

This document is disseminated under the sponsorship of the Department of Transportation in the interest of information exchange. The United States Government assumes no liability for its contents or use thereof.

NOTICE

The United States Government does not endorse products or manufacturers. Trade or manufacturers' names appear herein solely because they are considered essential to the objective of this report.

REPORT DOCUMENTATION PAGE*Form Approved
OMB No. 0704-0188*

Public reporting burden for this collection of information is estimated to average 1 hour per response, including the time for reviewing instructions, searching existing data sources, gathering and maintaining the data needed, and completing and reviewing the collection of information. Send comments regarding this burden estimate or any other aspect of this collection of information, including suggestions for reducing this burden, to Washington Headquarters Services, Directorate for Information Operations and Reports, 1215 Jefferson Davis Highway, Suite 1204, Arlington, VA 22202-4302, and to the Office of Management and Budget, Paperwork Reduction Project (0704-0188), Washington, DC 20503.

1. AGENCY USE ONLY (Leave blank)		2. REPORT DATE August 2010		3. REPORT TYPE AND DATES COVERED Technical Report	
4. TITLE AND SUBTITLE Locomotive Fuel Tank Structural Safety Testing Program: Passenger Fuel Tank Jackknife Derailment Load Test				5. FUNDING NUMBERS	
6. AUTHOR(S) Abdullatif K. Zaouk, Basant Parida, and Mark Silver					
7. PERFORMING ORGANIZATION NAME(S) AND ADDRESS(ES) Foster-Miller, Inc. (subsidiary of QinetiQ North America) 350 Second Avenue Waltham, MA 02451-1196				8. PERFORMING ORGANIZATION REPORT NUMBER	
9. SPONSORING/MONITORING AGENCY NAME(S) AND ADDRESS(ES) U.S. Department of Transportation Federal Railroad Administration Office of Research and Development 1200 New Jersey Avenue, SE Washington, DC 20590				10. SPONSORING/MONITORING AGENCY REPORT NUMBER DOT/FRA/ORD-10/08	
11. SUPPLEMENTARY NOTES Program Manager: John Punwani					
12a. DISTRIBUTION/AVAILABILITY STATEMENT This document is available to the public through the FRA Web site at http://www.fra.dot.gov .				12b. DISTRIBUTION CODE	
13. ABSTRACT (Maximum 200 words) This report presents the results of a passenger locomotive fuel tank load test simulating jackknife derailment (JD) load. The test is based on FRA requirements for locomotive fuel tanks in the Title 49, Code of Federal Regulations (CFR), Part 238, Appendix D. This test covers Section (a) (2) of Appendix D, which states that the fuel tank shall support transversely at the center a sudden loading equivalent to one-half the weight of the locomotive at a vertical acceleration of 2g without exceeding the ultimate strength of the material. The load is assumed to be supported by one rail, distributed between the longitudinal centerline and the edge of the tank bottom, with a railhead surface of 2 inches (in). The nominal weight of an F59 PHI passenger locomotive is approximately 268,000 pounds (lb). This report presents the test data and their correlations to the results of finite element analysis (FEA) using ABAQUS. The test data showed that the resulting vertical displacement of the tank bottom wall corresponding to a maximum JD load of 317 kilopounds was approximately 4 in. This comprised both elastic and plastic components of deformation. Upon unloading, a local residual plastic deformation of nearly 1 in was found, and no crack or breach in the tank wall was detected in the plastically deformed zone or elsewhere. Results of FEA are also included and compared with those obtained from the test. From the FRA regulatory perspective, the tank is considered to have satisfied the structural integrity requirements set forth in CFR 49, Part 238, Appendix D, Section (a) (2).					
14. SUBJECT TERMS Passenger locomotive fuel tank, jackknife derailment load condition				15. NUMBER OF PAGES 49	
				16. PRICE CODE	
17. SECURITY CLASSIFICATION OF REPORT Unclassified	18. SECURITY CLASSIFICATION OF THIS PAGE Unclassified	19. SECURITY CLASSIFICATION OF ABSTRACT Unclassified	20. LIMITATION OF ABSTRACT Unlimited		

NSN 7540-01-280-5500

Standard Form 298 (Rev. 2-89)
Prescribed by ANSI Std. Z39-18
298-102

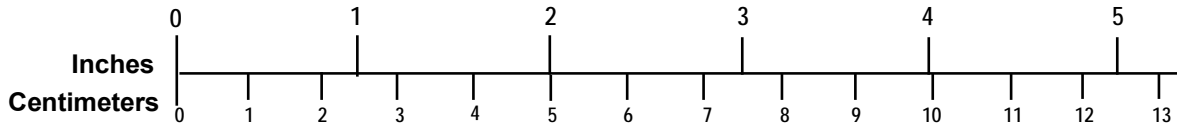
METRIC/ENGLISH CONVERSION FACTORS

ENGLISH TO METRIC

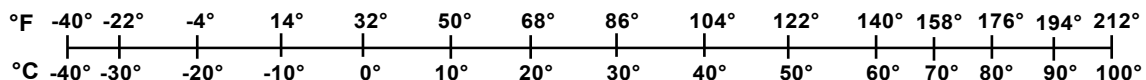
METRIC TO ENGLISH

<p>LENGTH (APPROXIMATE)</p> <p>1 inch (in) = 2.5 centimeters (cm)</p> <p>1 foot (ft) = 30 centimeters (cm)</p> <p>1 yard (yd) = 0.9 meter (m)</p> <p>1 mile (mi) = 1.6 kilometers (km)</p>	<p>LENGTH (APPROXIMATE)</p> <p>1 millimeter (mm) = 0.04 inch (in)</p> <p>1 centimeter (cm) = 0.4 inch (in)</p> <p>1 meter (m) = 3.3 feet (ft)</p> <p>1 meter (m) = 1.1 yards (yd)</p> <p>1 kilometer (km) = 0.6 mile (mi)</p>
<p>AREA (APPROXIMATE)</p> <p>1 square inch (sq in, in²) = 6.5 square centimeters (cm²)</p> <p>1 square foot (sq ft, ft²) = 0.09 square meter (m²)</p> <p>1 square yard (sq yd, yd²) = 0.8 square meter (m²)</p> <p>1 square mile (sq mi, mi²) = 2.6 square kilometers (km²)</p> <p>1 acre = 0.4 hectare (he) = 4,000 square meters (m²)</p>	<p>AREA (APPROXIMATE)</p> <p>1 square centimeter (cm²) = 0.16 square inch (sq in, in²)</p> <p>1 square meter (m²) = 1.2 square yards (sq yd, yd²)</p> <p>1 square kilometer (km²) = 0.4 square mile (sq mi, mi²)</p> <p>10,000 square meters (m²) = 1 hectare (ha) = 2.5 acres</p>
<p>MASS - WEIGHT (APPROXIMATE)</p> <p>1 ounce (oz) = 28 grams (gm)</p> <p>1 pound (lb) = 0.45 kilogram (kg)</p> <p>1 short ton = 2,000 pounds (lb) = 0.9 tonne (t)</p>	<p>MASS - WEIGHT (APPROXIMATE)</p> <p>1 gram (gm) = 0.036 ounce (oz)</p> <p>1 kilogram (kg) = 2.2 pounds (lb)</p> <p>1 tonne (t) = 1,000 kilograms (kg) = 1.1 short tons</p>
<p>VOLUME (APPROXIMATE)</p> <p>1 teaspoon (tsp) = 5 milliliters (ml)</p> <p>1 tablespoon (tbsp) = 15 milliliters (ml)</p> <p>1 fluid ounce (fl oz) = 30 milliliters (ml)</p> <p>1 cup (c) = 0.24 liter (l)</p> <p>1 pint (pt) = 0.47 liter (l)</p> <p>1 quart (qt) = 0.96 liter (l)</p> <p>1 gallon (gal) = 3.8 liters (l)</p> <p>1 cubic foot (cu ft, ft³) = 0.03 cubic meter (m³)</p> <p>1 cubic yard (cu yd, yd³) = 0.76 cubic meter (m³)</p>	<p>VOLUME (APPROXIMATE)</p> <p>1 milliliter (ml) = 0.03 fluid ounce (fl oz)</p> <p>1 liter (l) = 2.1 pints (pt)</p> <p>1 liter (l) = 1.06 quarts (qt)</p> <p>1 liter (l) = 0.26 gallon (gal)</p> <p>1 cubic meter (m³) = 36 cubic feet (cu ft, ft³)</p> <p>1 cubic meter (m³) = 1.3 cubic yards (cu yd, yd³)</p>
<p>TEMPERATURE (EXACT)</p> <p>$[(x-32)(5/9)]\text{ }^{\circ}\text{F} = y\text{ }^{\circ}\text{C}$</p>	<p>TEMPERATURE (EXACT)</p> <p>$[(9/5)y + 32]\text{ }^{\circ}\text{C} = x\text{ }^{\circ}\text{F}$</p>

QUICK INCH - CENTIMETER LENGTH CONVERSION



QUICK FAHRENHEIT - CELSIUS TEMPERATURE CONVERSION



For more exact and or other conversion factors, see NIST Miscellaneous Publication 286, Units of Weights and Measures.
Price \$2.50 SD Catalog No. C13 10286

Updated 6/17/98

Acknowledgments

This report discusses full-scale passenger fuel tank test simulating a jackknife derailment loading condition. Foster-Miller, Inc. (FMI)/QinetiQ North America performed this work under contract number DTFR53-03-D-00002 from the Federal Railroad Administration (FRA) for the Locomotive Fuel Tank Safety Improvement Program.

John Punwani, FRA Office of Research and Development, is the contract officer's technical representative, and the authors thank him for his technical direction and involvement in the project.

The support of Claire Orth (retired), Chief of Equipment and Operating Practices, FRA Office of Research and Development, and of Dr. Magdy El-Sibaie, Former Director of the FRA Office of Research and Development, is gratefully acknowledged.

The authors would like to express their gratitude to Gopal Samavedam for his encouragement and guidance and wish to thank Norm Dana for the CAD drawings and John Kidd and John Flynn for help with test setup.

Contents

Executive Summary	1
1. Introduction	2
1.1 Background	2
1.2 Objectives	2
2. Technical Approach	3
2.1 Test Condition	3
2.2 Test Fixture	3
2.3 Fuel Tank Load Measurement Method	5
2.3.1 Load Lever Joint Force Calibration	6
2.4 Test Article	8
2.5 Test Instrumentation and Data Acquisition	9
2.6 Test Methodology	12
3. Test Results and Discussions	14
4. Results of Simulation and FEA	18
4.1 Mechanical Properties Evaluation of F59 Tank Material	18
4.1.1 Test Sample Preparation and Testing	18
4.1.2 Tensile Test Results	18
4.2 FEA	20
5. Conclusions	27
6. References	28
Appendix A. Summary of F59 Tank Material Tensile Properties Data	29
Abbreviations and Acronyms	41

Illustrations

Figure 1. Schematic of FRA JD Load on Tank Bottom Wall	3
Figure 2. Locomotive Fuel Tank Test Fixture	4
Figure 3. Test Fixture and Tank Configuration for JD Load Case	5
Figure 4. Schematic Test Setup for Fulcrum Calibration Test	6
Figure 5. Fulcrum Calibration Test Setup at FMI Tank Test Facility	7
Figure 6. External Dimensions of F59 PHI Passenger Locomotive Tank	8
Figure 7. F59 Tank Interior Details including Component Wall Thicknesses	9
Figure 8. Test Control and Data Acquisition System Setup	10
Figure 9. Closeup of Lateral Support and String Potentiometer Connection to Load Lever	11
Figure 10. String Potentiometer Attachment to the Top Wall of Inverted Tank	11
Figure 11. CAD Drawing of Test Setup for “JD” Load Case	13
Figure 12. Test Setup with a Strut Laterally Supporting the Load Lever.....	13
Figure 13. Jackknife Load vs. Vertical Displacement of Load Lever on Tank Bottom Wall	14
Figure 14. Jackknife Load vs. Tank Top Plate Vertical Displacement as a Result of Tank Bending	15
Figure 15. Undeformed Shape of Inverted Tank Bottom Wall in Contact with Rail before Test	16
Figure 16. Posttest Closeup View of Deformed F59 Tank Bottom Wall	17
Figure 17. Tensile Stress vs. Strain Curve for Tank Top Plate Material.....	19
Figure 18. Extracted True Stress vs. True Strain Data for Tank Top Plate Material.....	20
Figure 19. FEM of F59 Tank under JD Loading: (a) Inverted Tank and Load Lever and (b) a Cutaway View of Tank Internal Structure	21
Figure 20. Von Mises Stress Contours Corresponding to Applied Maximum Jackknife Load: (a) in the Bottom Wall of F59 Tank and (b) in the Internal Structures of Tank.....	23
Figure 21. Force vs. Displacement Data from FEA and Jackknife Load Test	24
Figure 22. Comparison of Localized and Distributed von Mises Stresses in FEM: (a) just before 2.5-Inch Vertical Displacement and (b) after 2.5-Inch Displacement....	25
Figure 23. A Cutaway View of FEM Showing von Mises Stress Distribution in the Buckled Components under the Load Lever	26

Tables

Table 1. Material Thickness and Properties Used in FEM for Key Components of F59 Tank 22

Executive Summary

As part of the Federal Railroad Administration (FRA) Fuel Tank Safety Improvement Program, the structural integrity of an F59 PHI passenger locomotive fuel tank was evaluated under “jackknife derailment” (“JD”) load case. The quasi-static load test was performed in a custom-designed fuel tank test fixture located at Foster-Miller, Inc. (FMI)/QinetiQ North America’s (QNA) Transportation Research Center (Fitchburg, MA). This report presents the details of the test setup, instrumentation, methodology, and results. Correlation of test results with those obtained from finite element analysis (FEA) by using ABAQUS is also shown.

The results of jackknife derailment load test reveal that the supplied F59 PHI tank is capable of withstanding a quasi-static load as specified by the Title 49, Code of Federal Regulations (CFR), Part 238, Appendix D, Section (a) (2), which states that the fuel tank shall support transversely at the center a sudden loading equivalent to one-half the weight of the locomotive at a vertical acceleration of 2g without exceeding the ultimate strength of the material. The load is assumed to be supported on one rail, distributed between the longitudinal centerline and the edge of the tank bottom, with a railhead surface of 2 inches (in). The nominal weight of F59 passenger locomotive is approximately 268,000 pounds (lb).

Test results showed that the bottom wall of the tank safely resisted the applied maximum load of 317,000 lb without fracture or cracking. The tank exhibited clear evidence of undergoing local plastic deformation in the contact region with the railhead attached to the load lever. The rest of the tank experienced elastic bending, but it was not damaged, as were the tank attachment fixtures. The results of simulation and FEA by using ABAQUS also confirmed that the resultant stress magnitude under applied maximum load did not reach the ultimate strength of tank material. Hence, from the FRA regulatory perspective, it is concluded that the tank passed the structural integrity requirement set forth in CFR 49, Part 238, Appendix D, Section (a) (2).

1. Introduction

1.1 Background

Ensuring the structural integrity of locomotive fuel tanks in railroad accidents is crucially important to improving the safety of train crews and passengers. Damage to tanks and associated fuel system components can lead to leaks, potential fires, and cause pollution, resulting in loss of property as well as passenger injuries. The FRA Fuel Tank Safety Improvement Program is being pursued to address these safety concerns.

FRA specified the loads a typical fuel tank must withstand for safety under jackknife derailment, minor derailment (MD), and side bumper load. Full-scale tests to validate passenger fuel tank strength resisting these loads following derailment have not been performed to date, except for a few tests on freight locomotive tanks in Fitchburg, MA, by FMI/QNA.

1.2 Objectives

The objectives of the test were as follows:

- (a) Simulate the jackknife loading condition on the F59 PHI passenger locomotive fuel tank on the full-scale test fixture built at the Transportation Research Center in Fitchburg;
- (b) Prepare the test setup with load cells and displacement transducers;
- (c) Determine the load versus displacement data identifying salient points related to plastic yielding, peak load, and displacement;
- (d) Determine the unloading behavior of the tank upon removal of the load;
- (e) Identify the permanent deflection in the tank bottom wall and cracking, if any; and
- (f) Correlate the test data with those obtained from FEA and explain reasons for discrepancies, if any.

2. Technical Approach

2.1 Test Condition

All primary locomotive fuel tanks are required to resist certain loading conditions without failure, per FRA regulations which incorporate American Association of Railroads (AAR) Standard S-5506, Performance Requirements for Diesel Electric Locomotive Fuel Tanks (October 1, 2001). These regulations originated through collaborative efforts of AAR and FRA, were introduced as Recommended Practice RP-506 for new manufacture in 1995, and have been used by the industry after that time as guidelines. In 2004, these were formally incorporated into the Title 49, CFR, Part 238. The requirements make up the application of three static load conditions by railhead surface or front bumper of a land vehicle to the tank exterior, representing exposure to three different accident scenarios, namely minor derailment (MD), jackknife derailment (JD), and the side impact (SI) loading. This report covers the test condition involving JD, the jackknife derailment case, only.

This test covers Section (a) (2) of Appendix D of CFR 49, Part 238 (FRA, 2005), which states that “the fuel tank shall support transversely at the center a sudden loading equivalent to one-half the weight of the locomotive at a vertical acceleration of 2g, without exceeding the ultimate strength of the material. The load is assumed to be supported on one rail, distributed between the longitudinal centerline and the edge of the tank bottom, with a railhead surface of two inches.” The nominal weight of an F59 PHI passenger locomotive is approximately 268,000 lb. This represents one of the severe loading cases of a derailed locomotive straddled across the rail, with only one rail supporting the complete locomotive weight on half the tank width, as shown in Figure 1.

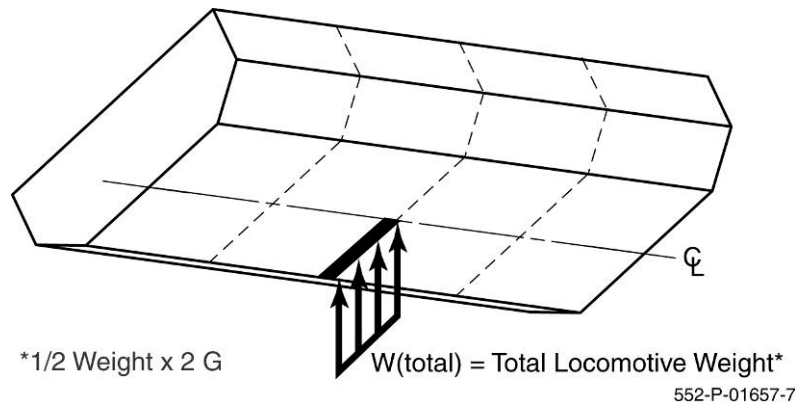


Figure 1. Schematic of FRA JD Load on Tank Bottom Wall

2.2 Test Fixture

FMI/QNA performed the test outlined in this document by using the fuel tank test fixture illustrated in Figure 2. The test fixture was custom-designed and developed by FMI/QNA to test a fuel tank in all standard derailment configurations and is located at its Fitchburg Transportation Research Center in Massachusetts. The modular nature of the fixture allows for different tank types to be tested in multiple load configurations with minimal modifications.

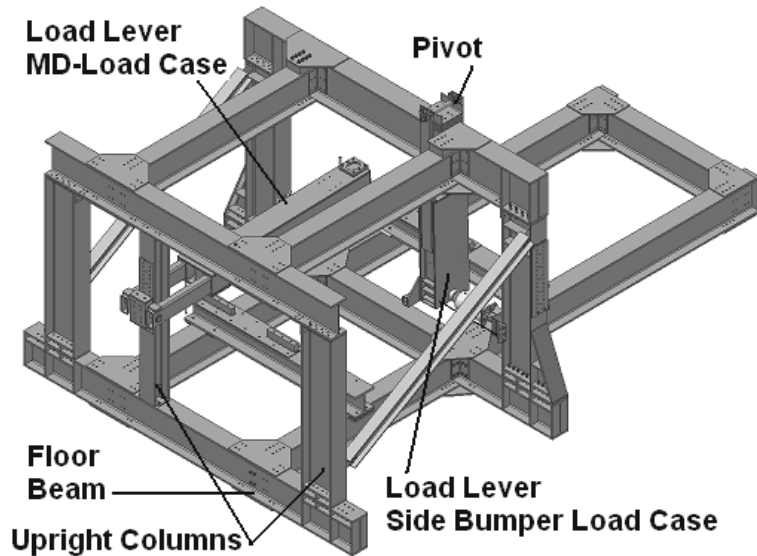


Figure 2. Locomotive Fuel Tank Test Fixture

The fixture was designed to enable application of all three types of FRA derailment load conditions to a wide range of full-size production locomotive fuel tanks. The tanks are tested upside-down relative to their position in actual locomotives. Movable support beams are used to reposition tanks relative to the loading levers, which contain a segment of actual rail or bumpers making contact with the tank. The levers swing in large-radius arcs to closely reflect the translational movement of the railhead or bumper into the tank implied by the regulations. Use of widely spaced supports and stiff lever arms were made to ensure stability of the fixture under unpredictable crushing behavior, which might occur when large deflections (6–8 in) are produced on the tank walls. The test fixture is therefore capable of stable operation under these extreme loading conditions.

The tank support brackets are also accommodated, because these are part of the tank attachment system and are also subjected to the impact loads. The tests therefore tax these important components, because they must function satisfactorily under the required load conditions.

Figure 3 shows the test fixture and fuel tank setup configuration for application of FRA JD load to the F59 passenger locomotive fuel tank.

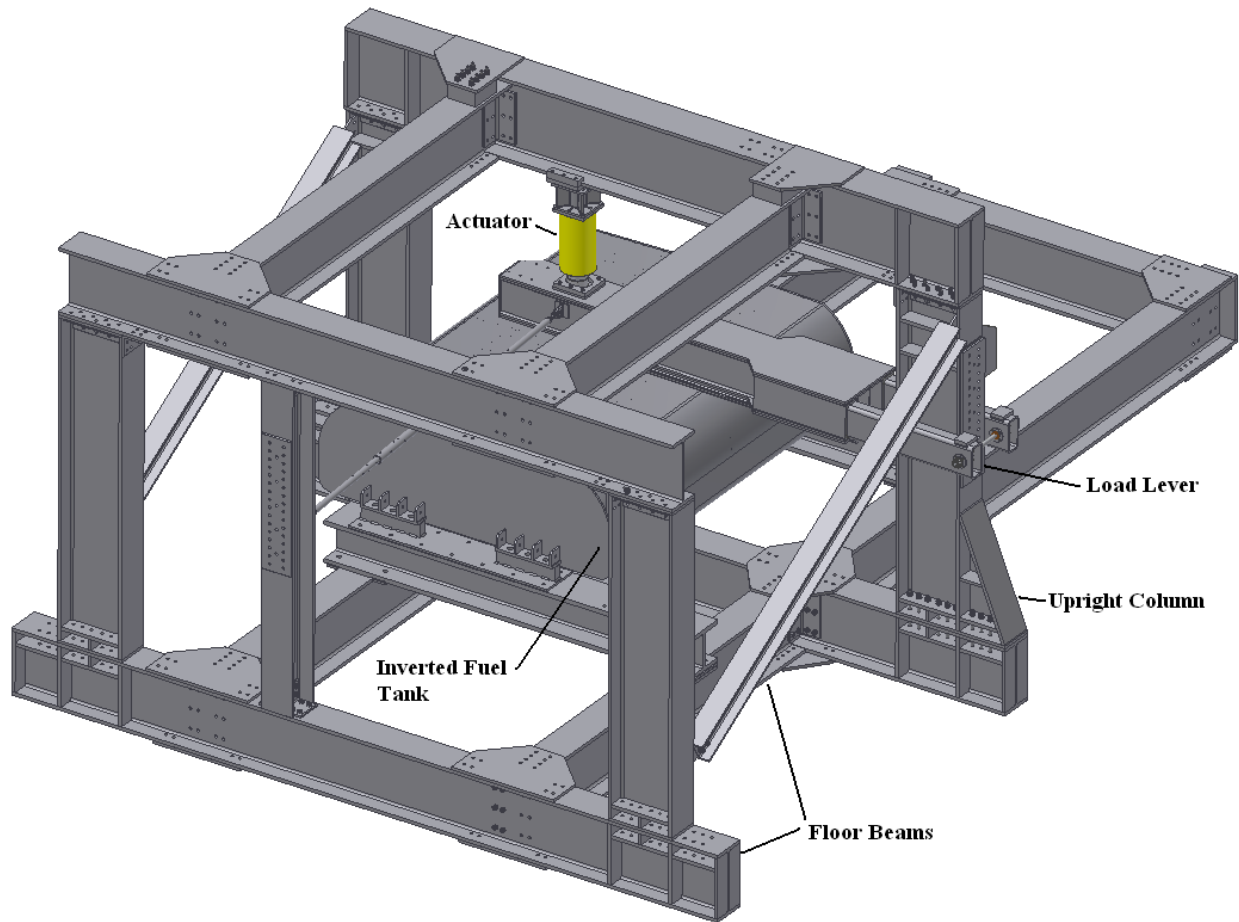


Figure 3. Test Fixture and Tank Configuration for JD Load Case

Initially shakedown testing was conducted to prove out the integrity of test fixture and instrumentation and to refine test procedures. Additionally, a separate calibration test was performed for the assessment of pivot joint reaction force of the load lever.

2.3 Fuel Tank Load Measurement Method

The total fuel tank reaction load in the JD loading test mode is composed of the main hydraulic actuator load acting on the load lever, the vertical reaction force at the far end of the lever (the vertical “pivot load”), and the weight fraction of the load lever assembly itself (approximate total weight of 5,000 lb).

To accurately estimate the vertical reaction force acting at the far end of the load lever at the pivot point, two 200-kilopound (kip)-capacity compression load cells were used on either side of the lever just above the pivot pin, as shown in Figure 4. The sum of the output of these two cells under tank loading provides the resultant vertical reaction force J at the pivot joint.

Figure 4 shows the forces and reactions acting between load lever and tank in a typical JD load test. Equilibrium of vertical forces shows that the load lever pivot reaction plus the hydraulic actuator load would equal the total load applied to the tank, which is the total fuel tank reaction force. The location of the resultant force acting on the tank bottom can also be obtained through

quasi-static moment equilibrium equation. This is described in detail in Section 2.3.1, which also provides the calibration method designed to determine the magnitude of pivot reaction force necessary in testing of the tank subjected to JD load.

2.3.1 Load Lever Joint Force Calibration

The purpose of the load lever joint force calibration with the help of a fulcrum is to let us calculate the pivot joint load and complete the information for determining the total load applied by the lever on the tank and its effective center of effort. The hydraulic actuator load and weight of the load lever, including rail section, are known parameters. The calibration test was set up and performed as depicted in Figure 4 and Figure 5. A known vertical shear force is applied to the lever beam by using an intermediate fulcrum on the test bed (without the tank), where P is the hydraulic actuator load, W the load lever weight, J the reaction force on the lever arm at the pivot joint, and F the resultant force at the fulcrum.

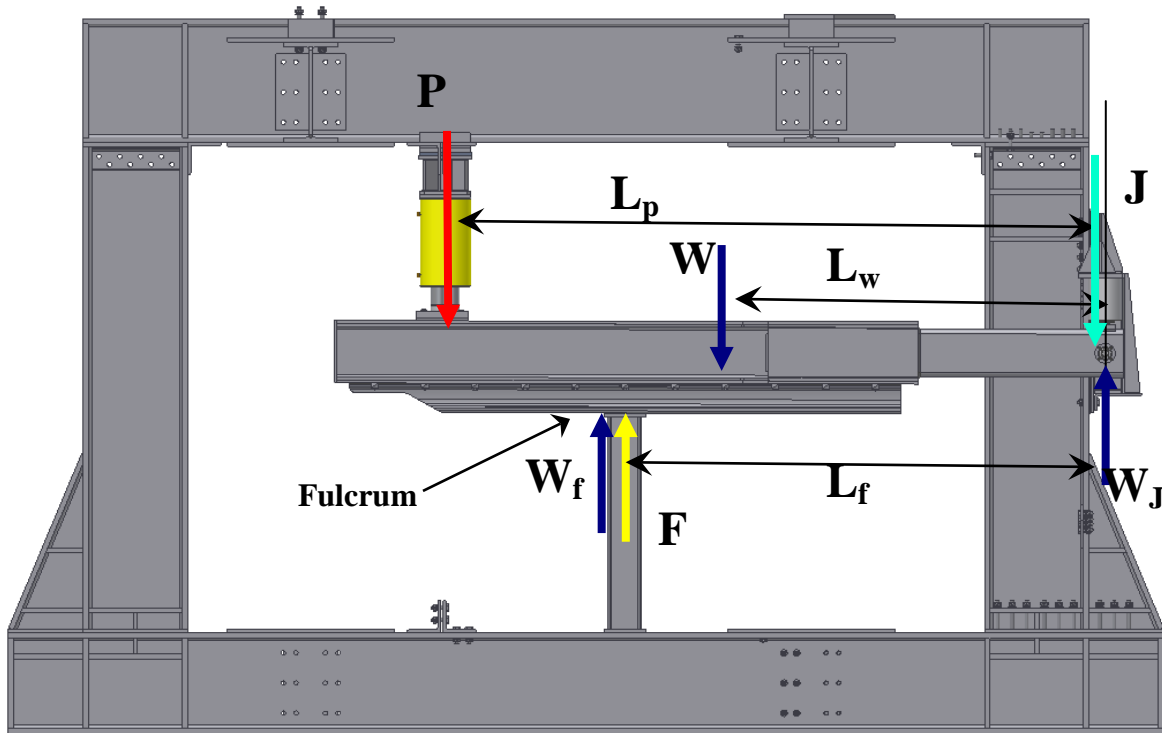


Figure 4. Schematic Test Setup for Fulcrum Calibration Test



Figure 5. Fulcrum Calibration Test Setup at FMI Tank Test Facility

From the free-body diagram of the load lever and sum of all vertical forces and reactions acting on it as shown in Figure 4,

$$P + W + J - F - (W_f + W_j) = 0 \quad (1)$$

where

- W_f is the reaction force at the fulcrum to the lever arm weight fraction = $W \cdot (L_w/L_f)$,
- W_j is the reaction force at pivot joint to the lever arm weight fraction = $W \cdot (L_f - L_w)/L_f$,
- L_p is the distance from the pivot axis to the center of the actuator,
- L_w is the distance from the pivot axis to the lever arm center of gravity, and
- L_f is the distance from pivot axis to the center of fulcrum.

However, the sum of the reaction forces W_f and W_j is equal to lever weight W , so Equation 1 can be rewritten as:

$$F = P + J \quad (2)$$

Taking the sum of the moments about the pivot axis to be zero and considering reaction to the weight fraction of the lever at fulcrum location to be $(W \cdot L_w/L_f)$, the fulcrum force F and pivot joint vertical force J can be computed from the following equations:

$$(P \cdot L_p) + (W \cdot L_w) - (F \cdot L_f) - \{(W \cdot L_w/L_f) \cdot L_f\} = 0 \quad (3)$$

$$\text{or the fulcrum force as a result of applied forces and reactions } F = P \cdot (L_p/L_f) \quad (4)$$

The vertical reaction force at pivot joint J due to applied actuator force P can be determined from Equation 2 as:

$$J = (F - P) = P \cdot \{(L_p/L_f) - 1\} \quad (5)$$

As previously mentioned, the vertical reaction force of the pivot joint is measured by using two load cells mounted above the two load lever arms (on both sides of the upright column supporting the pivot joint). This design feature also offered better stability and protection against lateral rotation of the lever about its longitudinal axis during the loading/deformation process. However, to constrain movement of the load lever to the vertical plane, an adjustable-length strut was attached to its side to offer lateral support to the lever during loading.

During the calibration test, the actuator force was gradually increased in steps, and the corresponding load cell readings were recorded. After the calibration test, the measured values of the pivot reaction forces J were found to be consistent with those computed from the above equations.

2.4 Test Article

The test article used in this testing program is an F59 PHI passenger locomotive fuel tank. This is reportedly manufactured by using strong corrosion-resistant (COR-TEN) steel material. Its overall shape and major external dimensions are shown in Figure 6. The interior construction details including baffle configurations and wall thicknesses are shown in Figure 7.

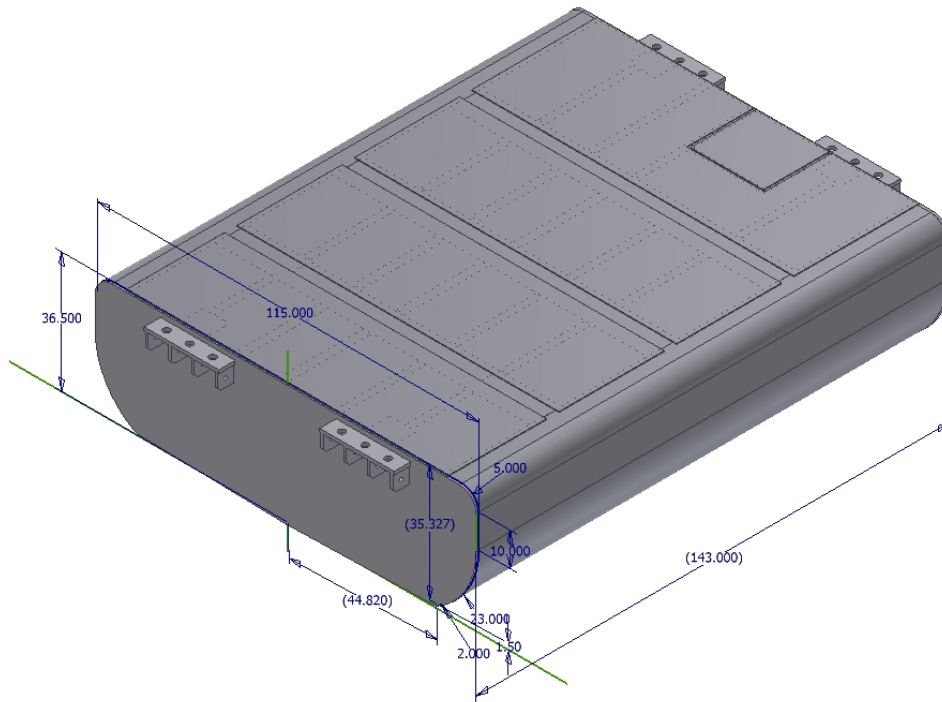


Figure 6. External Dimensions of F59 PHI Passenger Locomotive Tank

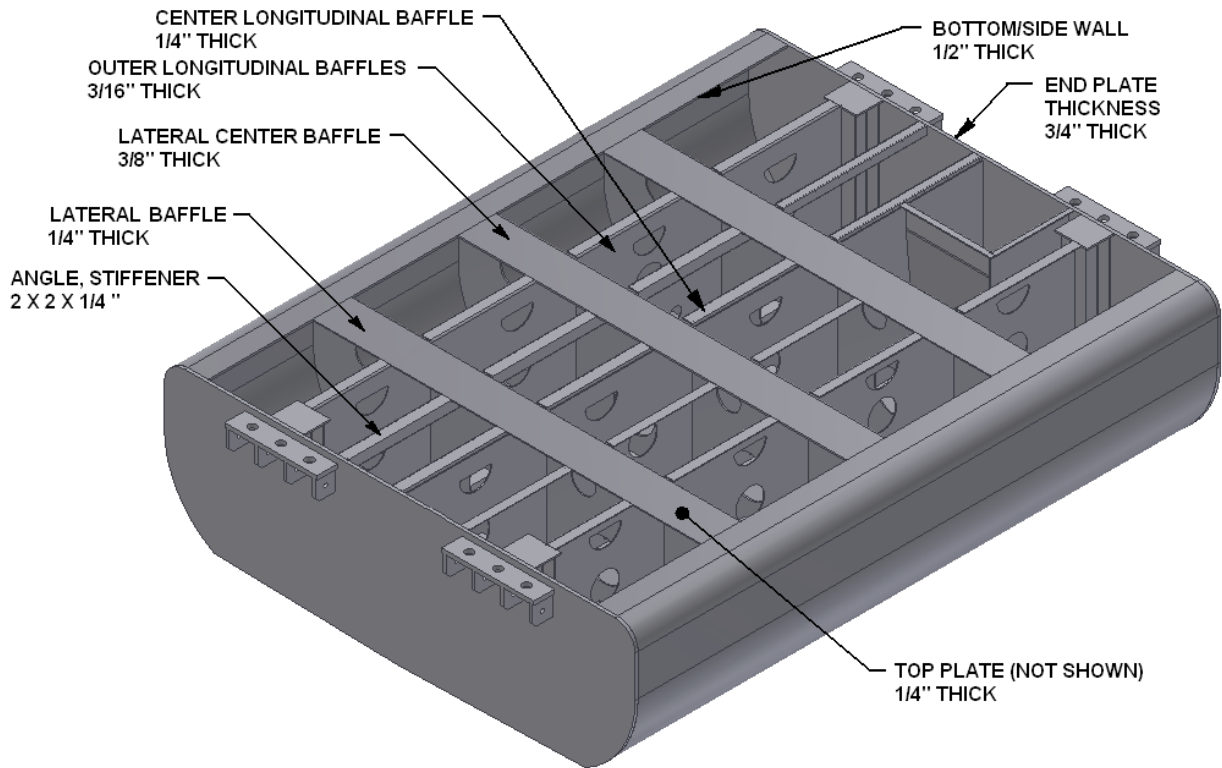


Figure 7. F59 Tank Interior Details including Component Wall Thicknesses

The JD load is intended to be applied at the longitudinal center of the fuel tank. However, considering the presence of a lateral center baffle thickest among all three lateral baffles (three-eighths-inch thick), the lever was shifted slightly outward so the load could be applied parallel to the lateral baffles and in between the center baffle and a one-quarter-inch lateral baffle. This would permit evaluation of tank structural integrity under worst-case JD load conditions.

2.5 Test Instrumentation and Data Acquisition

All test data for the fuel tank structural improvement program were acquired through National Instruments (NI) signal conditioners integrated with a high-end PC (Figure 8) using Laboratory Virtual Instrumentation Engineering Workbench (LabVIEW) version 8.2.1 software (NI, 2008a). LabVIEW is a graphical programming environment for measurement and automation developed by NI.



Figure 8. Test Control and Data Acquisition System Setup

In addition, the following instrumentation was used in this test:

Applied Load Instrumentation

Load is applied through an Enerpac hydraulic cylinder with a maximum capacity of 10,000 pounds per square inch (psi). To determine the applied actuator load a calibrated Setra 201 pressure transducer with a maximum pressure rating of 10,000 psi was used. This permits continuous monitoring of the pressure as well as applied actuator load data using LabVIEW software for data acquisition, reduction, and recording for later processing.

Pivot Reaction Force Instrumentation

For accurate pivot reaction force measurement, two calibrated BLH Model C2P1 200-kilopound compression load cells were mounted in an inverted position just above the pivot axis, as described in the previous section. The load cells were connected to an NI SCXI-1121 signal conditioner (NI, 2008a) with its output connected to the data acquisition PC.

Tank Deformation Instrumentation

To measure the tank bottom wall's vertical deformation because of JD load applied by the load lever, a Celesco string potentiometer was attached to the lever as shown in Figure 9. Two additional Celesco string pots were attached to the unloaded (inverted) top wall of F59 tank in the plane of transverse loading. These string pots were mounted symmetrically with respect to the central longitudinal baffle of the tank so as to measure the overall vertical deformation. The string potentiometer attachments between the top wall of the inverted tank and a transverse floor beam are shown in Figure 10. All three string pots were connected to an NI SCXI-1121 signal conditioning module.

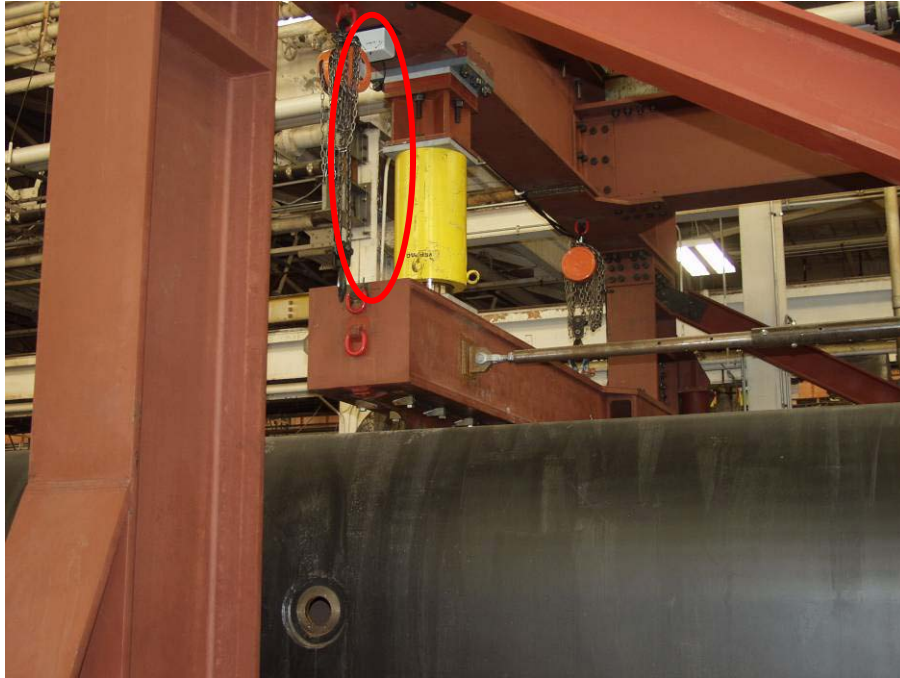


Figure 9. Closeup of Lateral Support and String Potentiometer Connection to Load Lever



Figure 10. String Potentiometer Attachment to the Top Wall of Inverted Tank

All test data were acquired through NI signal conditioners integrated with a high-end PC by using LabVIEW version 8.2.1 with NI-Daq 4.3 software (NI, 2008b), which permitted data acquisition, real-time display, and recording of data for later analysis (Figure 8).

2.6 Test Methodology

The test methodology for conducting JD load case comprised the following steps:

- The F59 tank was inverted upside down so that normal load could be applied to the tank bottom wall from the top with the help of a segment of railhead attached to the load lever.
- The tank support beams were moved as required to reposition the tank relative to the loading lever, which was determined from the drawing of test setup shown in Figure 3. Two support beams were anchored to the test rig, and the inverted tank was attached to the beams with fixtures at both ends of the tank.
- The load lever subassembly was moved and attached to the upright post of the test rig that was designed for the JD load case.
- Two 200-kip capacity load cells were aligned and attached in inverted position just above the pivot pin centerline, while the free end of the unloaded lever arm rested almost horizontally over the inverted tank at a position per the drawing in Figure 11.
- One end of an adjustable-length lateral support strut was attached to one side (web) of the load lever and the other end to the nearest upright post of the test rig. The length of this strut was adjusted to offer strong lateral support to the lever against sidewise movement or rotation (see Figure 12).
- The hydraulic actuator was positioned and attached to the designated transverse beam of the test fixture so that the piston of the actuator at minimum travel position made contact with the top surface of the load lever under an unloaded condition.
- One string potentiometer was attached between the load lever and the top transverse beam of the test rig, as shown in Figure 9. Two more string pots were attached between the bottom (top wall) of the inverted tank and a floor beam of the test rig as shown in Figure 10.
- The hydraulic hoses of the actuator were connected to the power pack, and the outputs of all transducers such as load cells, pressure transducer, and potentiometers were connected to the NI data acquisition hardware.
- The output of NI-Daq modules was connected to a high-end PC, loaded with LabVIEW version 8.2 software for real-time display of all transducer output data and for recording data to the hard disk.
- To begin the test, all calibrated transducers were reset to show zero output without load.
- A hydraulic power pack was started, and its pressure increased in steps to apply desired actuator load on the load lever.
- The maximum load applied to the tank was gradually raised beyond the weight of a passenger locomotive as stated under test condition in conformity with JD load specified under FAR regulations. All transducer output data were automatically recorded at a sampling rate of 1 kilohertz.
- The applied actuator load was gradually reduced to zero, and the residual vertical displacement of the tank bottom wall in the vicinity of initial railhead contact area was noted.

- Photographs of the deformed bottom wall of the tank were taken following test completion and lifting of load lever from tank surface with the help of a chain pulley.

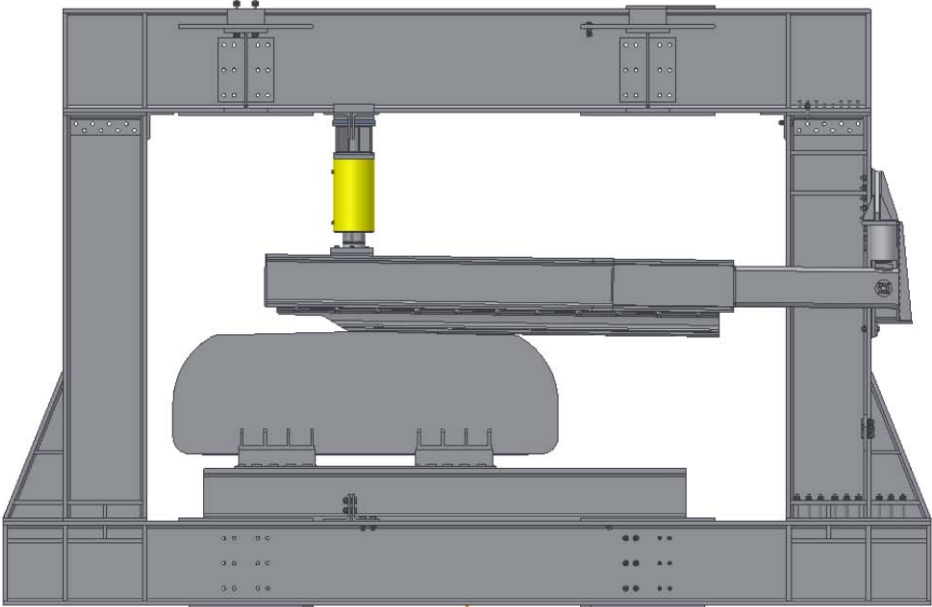


Figure 11. CAD Drawing of Test Setup for “JD” Load Case



Figure 12. Test Setup with a Strut Laterally Supporting the Load Lever

3. Test Results and Discussions

The JD load test followed the procedure outlined in Section 2.6. During the test, the resultant load from the lever on the bottom wall of the inverted F59 tank was the sum of the applied actuator load and the joint load at the pivot of load lever. The joint load was the sum of two load cells' output. The load point vertical displacement was determined from the output of the string potentiometer connected to the load lever at its initial contact position with the tank surface. The variation of applied actuator load, as well as the resultant jackknife load on the inverted tank and consequent vertical displacements of the lever in contact with tank bottom wall, is shown in Figure 13. The magnitude of joint load at the pivot joint of the lever is also shown in Figure 13.

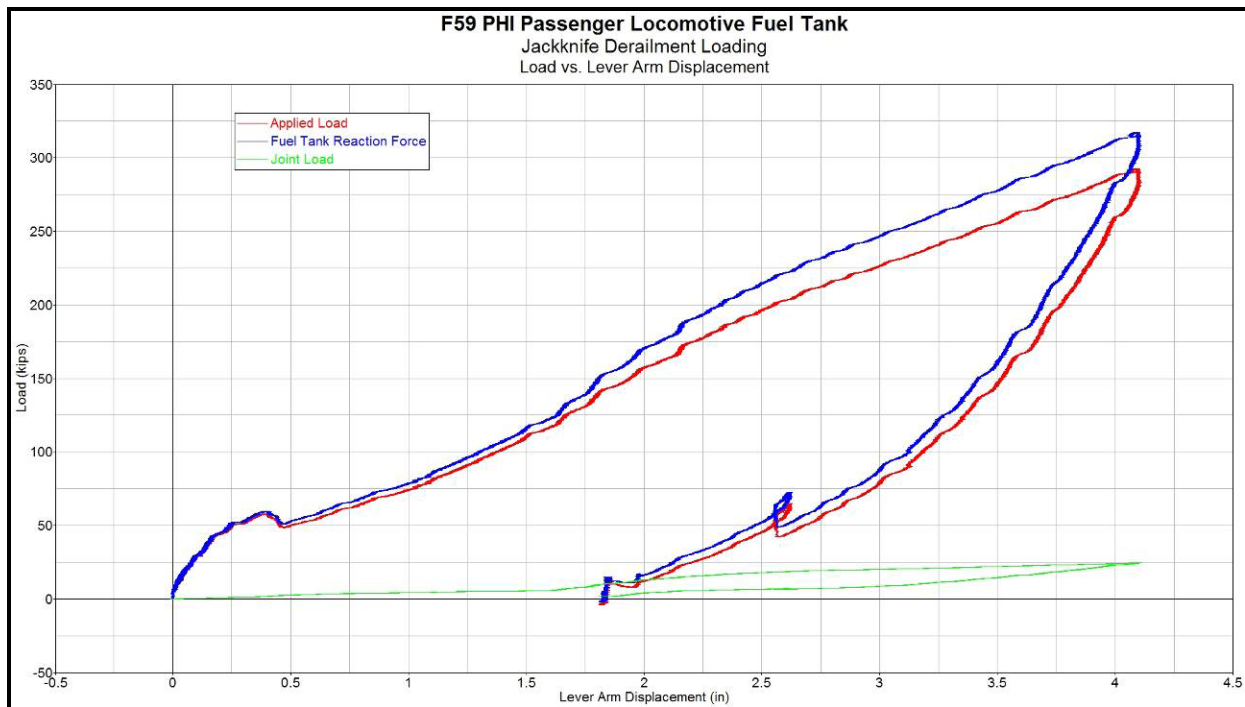


Figure 13. Jackknife Load vs. Vertical Displacement of Load Lever on Tank Bottom Wall

Following FRA guidelines for test conditions outlined in Section 2.4, the magnitude of applied load was increased up to and beyond 268 kip, the nominal weight of an F59 passenger locomotive. From Figure 13, it is observed that:

- At a total load of 268 kip, the vertical displacement was approximately 3.34 in.
- The maximum magnitude of resultant load applied was approximately 317 kip, and the corresponding vertical displacement was 4.1 in, with no failure or detectable cracking of the tank bottom wall.
- Following initial application of an approximately 60-kilopound load to the load lever, the tank bottom wall experienced an appreciable local deformation under the railhead contact point, as shown by slight drop in load at a vertical displacement of approximately 0.4 in.

- On continuation of loading, the deformed bottom wall of tank appeared to have effectively butted against the array of stiff baffles underneath (Figure 7).
- The railhead was in contact with the surface of the tank, enabling the total load on it to monotonically increase up to a maximum value of 317,129 lb.
- The maximum vertical displacement of the load lever was 4.1 in, which made up both elastic and plastic deformation of the tank.
- Upon gradual unloading of the tank, the elastic part of the (vertical) displacement of the tank was recovered, which is found to be approximately 2.27 in from Figure 13. The remaining 1.83 in is the vertical plastic displacement of the tank bottom wall at the test section.

The vertical displacement behavior of the top wall/entire tank in the plane of loading, as measured by two string pots attached between the (inverted tank) top wall and a transverse floor beam, is shown in Figure 14. The displacement shown represents the mean reading of the two string potentiometers because of tank bending.

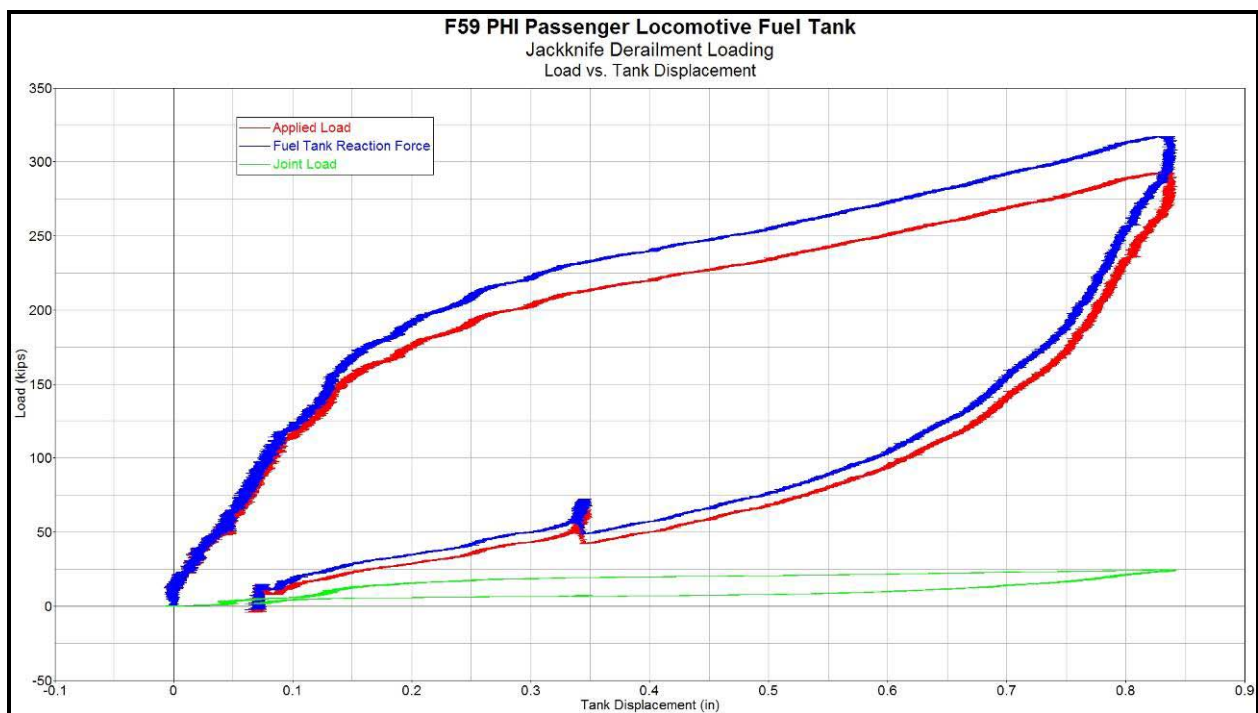


Figure 14. Jackknife Load vs. Tank Top Plate Vertical Displacement as a Result of Tank Bending

From Figure 14 it is observed that:

- The overall tank displacement behavior was nonlinear but nearly elastic, unlike the vertical displacement of the load lever in contact with the bottom wall of the inverted tank that exhibited a considerable local plastic deformation.

- The top plate of the tank in the plane of jackknife loading exhibited a maximum vertical displacement of only 0.84 in as a result of tank bending.
- Upon unloading from a maximum magnitude of 317 kip, the elastic bending displacement was completely recovered, which resulted in a small residual vertical displacement of less than 0.07 in.

From the analysis of results presented in Figure 13 and Figure 14, FMI/QNA concludes the following:

- The resulting vertical displacement of the tank bottom wall consisted of both elastic and plastic components. This was confirmed from the output of string potentiometers as well as from physical examination of the deformed wall surface, following complete unloading. The undeformed bottom wall and the deformed shape of it at the same location under the railhead are shown in Figure 15 and Figure 16, respectively.
- The presence of residual plastic deformation is clearly indicated in the vicinity of the railhead (attached to the load lever) contact with the tank bottom wall.
- The measured maximum value of the residual vertical displacement is 1.1 in, which is comparable to the 1.06 in obtained by subtracting the combined elastic displacements measured from Figure 13 and Figure 14, from the total displacement of 4.1 in at maximum test load.
- Once the elastic bending displacement of the entire tank in the plane of loading is taken into consideration, the maximum vertical displacement of tank bottom wall was actually 3.26 in at the maximum applied jackknife load of 317 kip.



Figure 15. Undeformed Shape of Inverted Tank Bottom Wall in Contact with Rail before Test



Figure 16. Posttest Closeup View of Deformed F59 Tank Bottom Wall

On the basis of these results, the supplied F59 PHI passenger locomotive tank demonstrated adequate strength against applied FRA JD load without any failure or breach in the walls of the tank. Furthermore, the load versus lever arm vertical displacement and the load versus tank bending displacement curves are suggestive of a greater load-bearing capacity of the tank. Therefore, the tested tank is considered to be safe against FRA-specified JD load.

4. Results of Simulation and FEA

4.1 Mechanical Properties Evaluation of F59 Tank Material

FMI/QNA carried out coupon-level material testing to obtain reliable properties, especially true stress versus true strain data for the components of the tank. These data were necessary as material input parameters for the FEA of the load case. Material testing was performed by fabricating F59 tank component specimens, machined to ASTM specifications, and by applying tensile load in an INSTRON test machine. The load is monotonically slowly increased (quasi-static loading) from its initial value of zero to its final value just before breaking so that the cross-section necking area and the corresponding tensile force could be measured for the computation of true stress. From the examination of the tensile stress in the specimen as a function of the strain, material properties such as the elastic modulus, yield stress, ultimate stress, and percent elongation at near-break condition of the components were obtained. Additionally, to represent sheet metal in ABAQUS, a linear isotropic plasticity material model was used. This material model required the true stress-strain relationship as input parameters for the postyield segment of the stress-strain curve. That necessitated generation of tensile properties data on small samples of plate materials obtained from various sheet metal components of the F59 PHI tank.

4.1.1 Test Sample Preparation and Testing

Initially, three tensile test coupons were made from small plate material cut from the fuel tank top plate. This was the only possible place to obtain test coupons. The thickness of the retrieved material from the top plate was 0.25 in. Therefore, three tensile test coupons were fabricated according to ASTM-E8 Standard for subsize coupons. However, test coupons were machined to be 6 in long to allow for use of an extensometer for accurate measurement of strain and percent elongation. The test coupons were tested in a calibrated INSTRON 1332 servo-hydraulic test machine. For consistency, the test machine crosshead-separation speed was maintained at 0.044 in/minute (min), and the data sampling rate was 300/min. An MTS extensometer with adequate range of travel was used to continuously monitor and record percent elongation of the gage section almost up to the breaking point. This feature of the test was useful in computation of true stress versus true strain deformation behavior of the material beyond its nominal ultimate stress point, which provided the necessary plastic strain component input into the ABAQUS FEA model.

4.1.2 Tensile Test Results

All the three identical coupons were tested in tension close to breaking point, and the results were found to be consistent. Figure 17 shows a sample tensile stress versus strain curve, plotted for engineering stress versus engineering strain. The results of all three test coupons showed that the average engineering yield stress of the material was 65,957 psi, the corresponding ultimate stress was 72,810 psi, and the average percent elongation at break was 21.7.

The test data were then used to compute the corresponding true stresses and true strains, based on the actual cross-section of the specimen, especially in the postyield regime associated with higher rate of elongation. With the assumption that there is no change to the total volume of the specimen gage section during the tensile test, the relationship between true and engineering stresses and strains can be derived as:

$$\sigma_T = \sigma_E (1 + \epsilon_E) \quad \dots\dots\dots (6)$$

$$\epsilon_T = \ln (1 + \epsilon_E) \quad \dots\dots\dots (7)$$

where σ_E and ϵ_E are engineering stresses and strains respectively and σ_T and ϵ_T are true stresses and true strains, respectively.

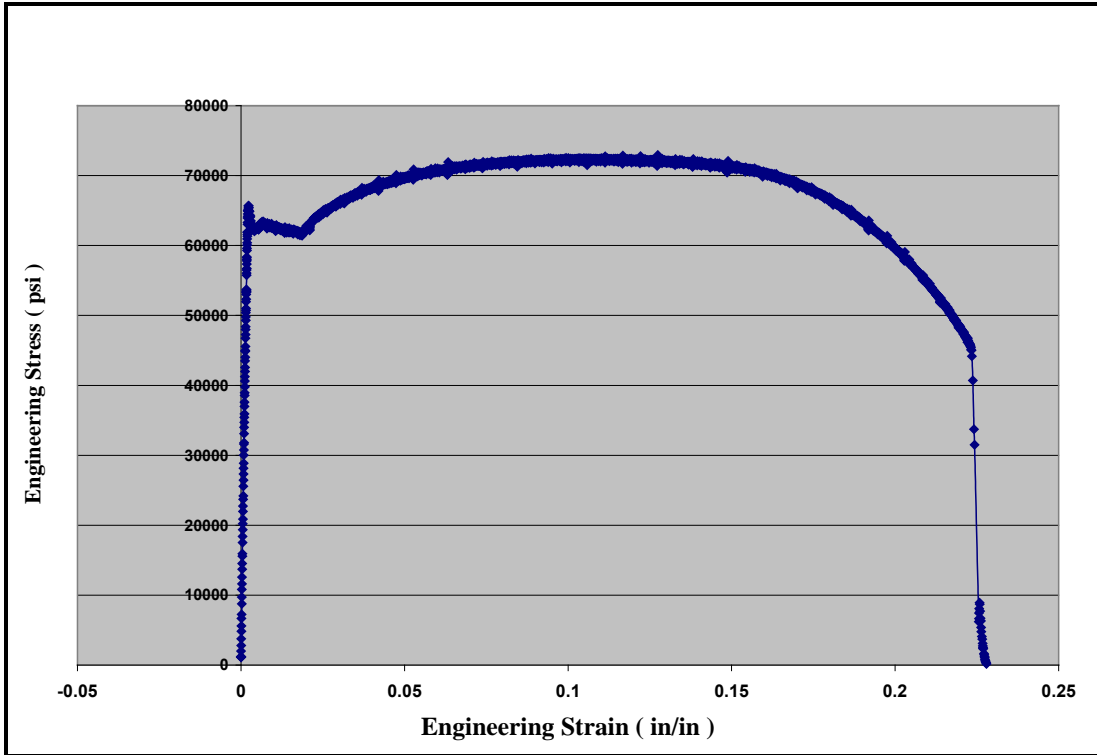


Figure 17. Tensile Stress vs. Strain Curve for Tank Top Plate Material

The computed true stress versus true strain data derived from data for a sample tensile test coupon is shown in Figure 18. In it the last point of the curve represents the true stress at the necking region of gage section, accurately computed by measuring actual cross-sectional dimensions of an unbroken specimen and with the known magnitude of applied load close to termination of test. For a failed specimen, the reconstituted cross-section necking area and the magnitude of tensile load just before its sudden drop at break were considered to compute the true stress, which offered the last data point of the test. Because the true stress magnitudes from necking and associated reduction in cross-section area increase beyond the ultimate stress point up to the breaking point, the interim true stress values were interpolated corresponding to true strain values. On the basis of the tensile test data of the tank top plate, it is believed to be made of high-strength low-alloy (HSLA) steel such as ASTM A 656 or A 715.

Subsequent to the completion of F59 tank testing for the MD and side impact load cases, small plate materials from other components of F59 were cut, tensile coupons fabricated and tested, and material properties similar to those of top plate were determined. The results of all those tests are included in the Appendix: Summary of F59 Tank Material Tensile Properties Data.

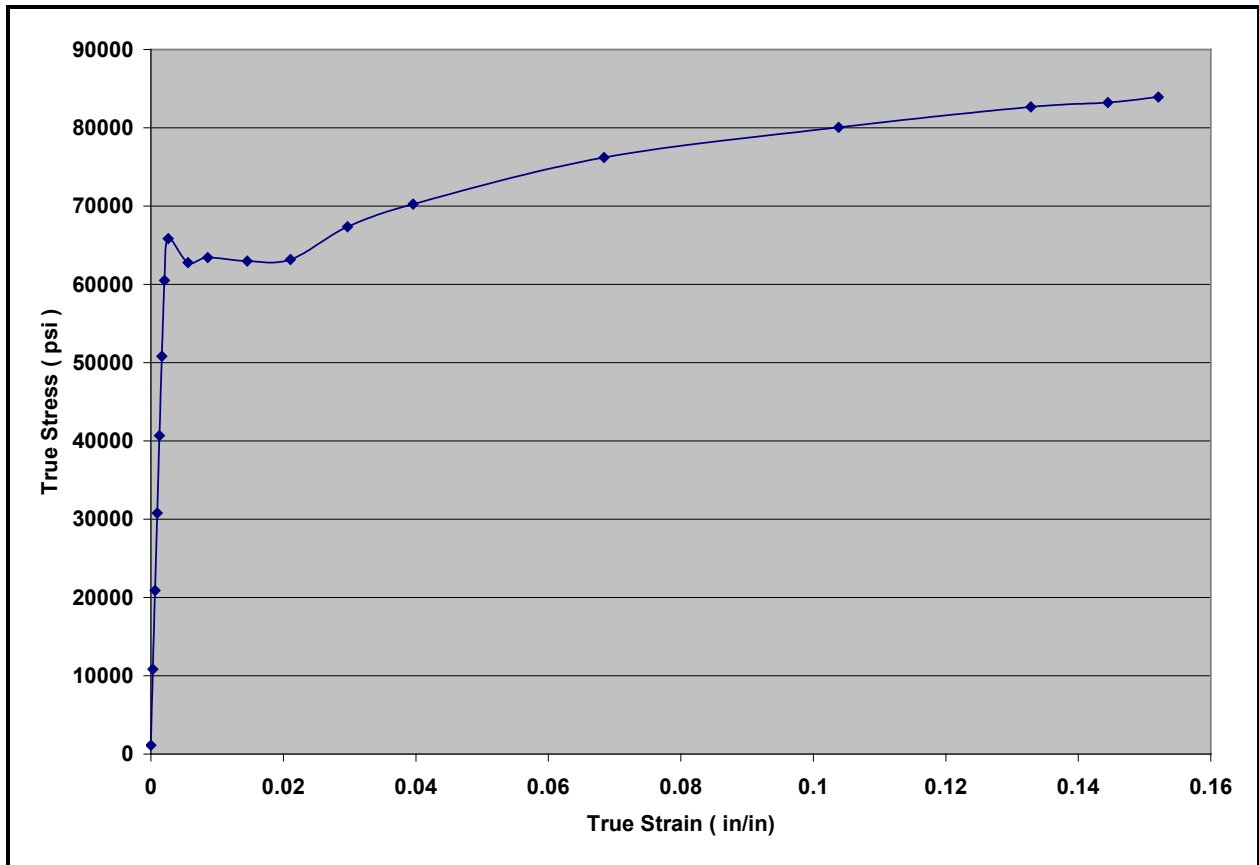


Figure 18. Extracted True Stress vs. True Strain Data for Tank Top Plate Material

4.2 FEA

A static finite element model (FEM) was developed in ABAQUS to model the jackknife derailment load case by using 95,459 shell and solid elements and kinematic constraints. The full model and the model with the bottom and sidewall elements removed to provide details of the internal components are shown in Figure 19 (a) and (b). Properties used in the model were determined from material test data of tank components. A summary of the material thickness and mechanical properties used in the FEM is shown in Table 1.

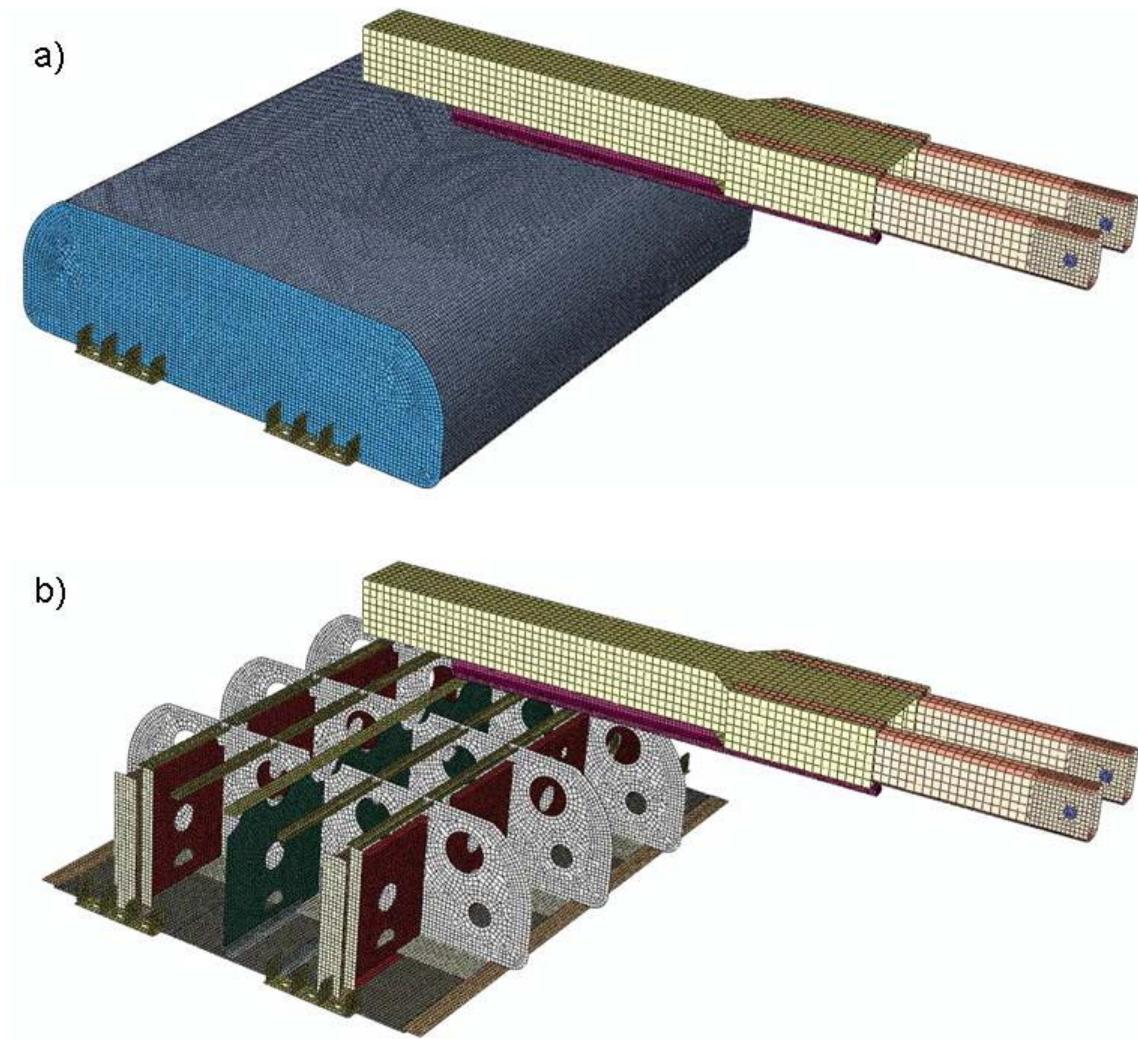


Figure 19. FEM of F59 Tank under JD Loading: (a) Inverted Tank and Load Lever and (b) a Cutaway View of Tank Internal Structure

Table 1. Material Thickness and Properties Used in FEM for Key Components of F59 Tank

Component	Thickness (in)	Material	Modulus (Msi)	Yield Stress (ksi)	Source
Top plate	0.25	HSLA Steel	30.5	65.9	Test
Bottom plate	0.491	CORTEN-B-QT70	29.4	70.4	Test
Side plates	0.491	CORTEN-B-QT70	29.4	70.4	Test
End plates	0.75	CORTEN-B	29.7	51.5	Test
Rail	n/a	High-strength steel	30.0	110.0	Handbook
Transverse baffles	0.3705	AISI 1030/CORTEN-A	29.5	50.9	Test
Longitudinal baffle (outer)	0.1825	CORTEN-A	28.7	50.1	Test
Longitudinal baffle (center)	0.2265	Cast iron	13.0	31.0	Test

Note: ksi, kilopound per square inch; Msi, million pounds per square inch.

The FEA predictions of von Mises stresses in F59 tank under applied maximum jackknife load condition and the corresponding load-point deformation behavior are shown in Figure 20 and Figure 21, respectively. The load/displacement history, analogous to that recorded from the corresponding full-scale tank test, was also determined in the FEM. These results are plotted together with the experimental data and shown in Figure 21. During the full-scale test for the JD case, the resultant peak load, including the load lever joint reaction force, had reached 317 kip, which was much higher than the required load of 268 kip per the FRA specification. Therefore, two load cases were analyzed in the FEM: one going up to the specified load of 268 kip and the other up to the maximum test load of 317 kip, including subsequent unloading to zero load in both cases. These results are shown, together with the resultant test data, in Figure 21.

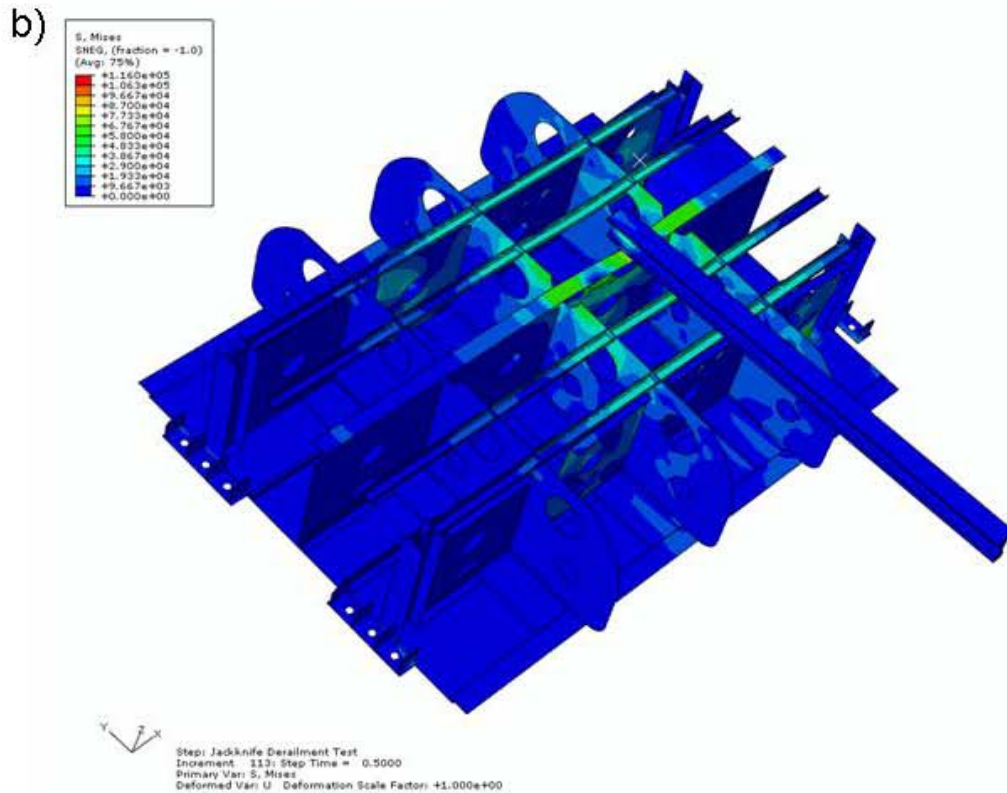
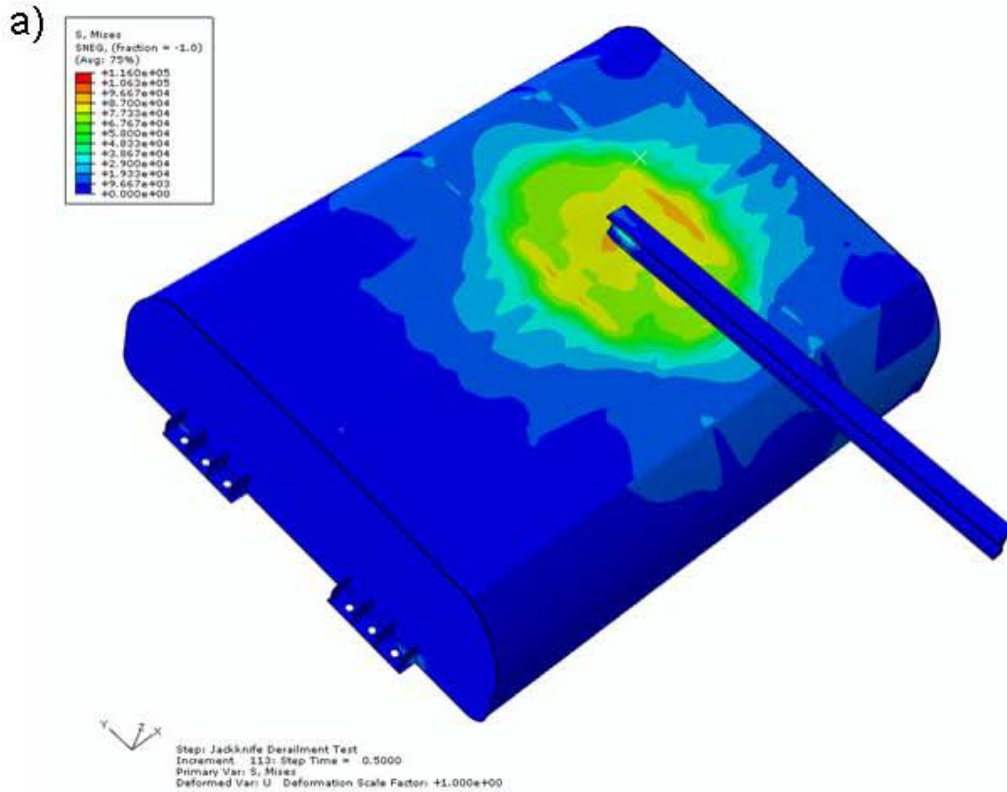


Figure 20. Von Mises Stress Contours Corresponding to Applied Maximum Jackknife Load: (a) in the Bottom Wall of F59 Tank and (b) in the Internal Structures of Tank

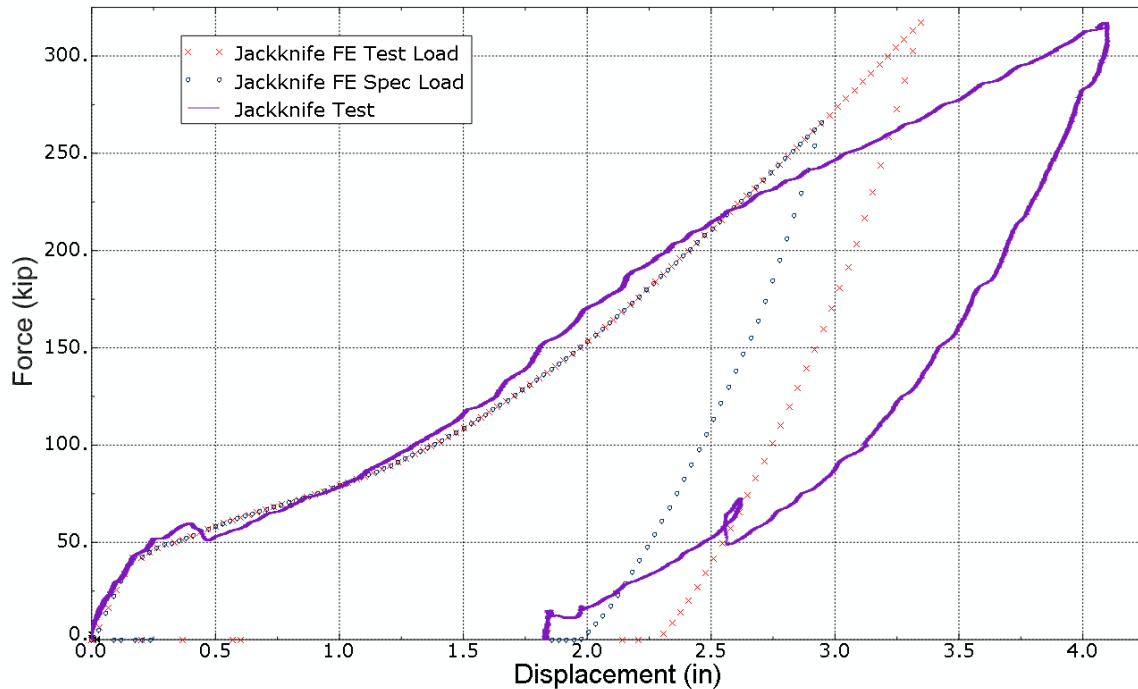


Figure 21. Force vs. Displacement Data from FEA and Jackknife Load Test

It is seen from Figure 21 that the FEA results generally agree well with the experimental data up to a vertical displacement of 2.5 in. Beyond this point, the FEM seems to offer higher stiffness compared with the actual test article, as is observable from the plotted data. This is most likely due to the inaccuracies in modeling of the joints among internal components, such as weld constraints or subcomponent material models throughout the FEM that become important in the large-deformation regime. During the transition from local stressing just under the point of load application to increasing stress distributions to the surrounding components of the fuel tank, proper characterization of joints and stiffness of connections plays an important role in accuracy of results. The von Mises stress contours obtained from the FEA just before and after this point in the analysis are shown in Figure 22 (a) and (b). A detailed depiction of the von Mises stress distribution corresponding to a peak vertical load of 317 kip is seen in a cutaway view of the model in Figure 23 that shows partially buckled internal components at the load application point. The welded seams everywhere in the model were modeled as rigid constraints. This was expected to provide a stiffer response of the tank to external loading than corresponding to an exact modeling of the welds. To investigate this modeling artifact, an attempt was made at modeling the welds as pinned connections, rather than rigid one. Doing so, however, introduced instability into the solution, and the model failed to converge.

However, if the maximum test load were restricted to 268 kip, as required by the FRA test condition for the JD case, the FEM results would agree more closely with the experimental results. The response of the structure to loads greater than the specified magnitude and the consequent larger vertical deformation of the bottom plate and associated internal structure would require more

elaborate modeling methods, including full knowledge of the welding materials and type of welding used throughout.

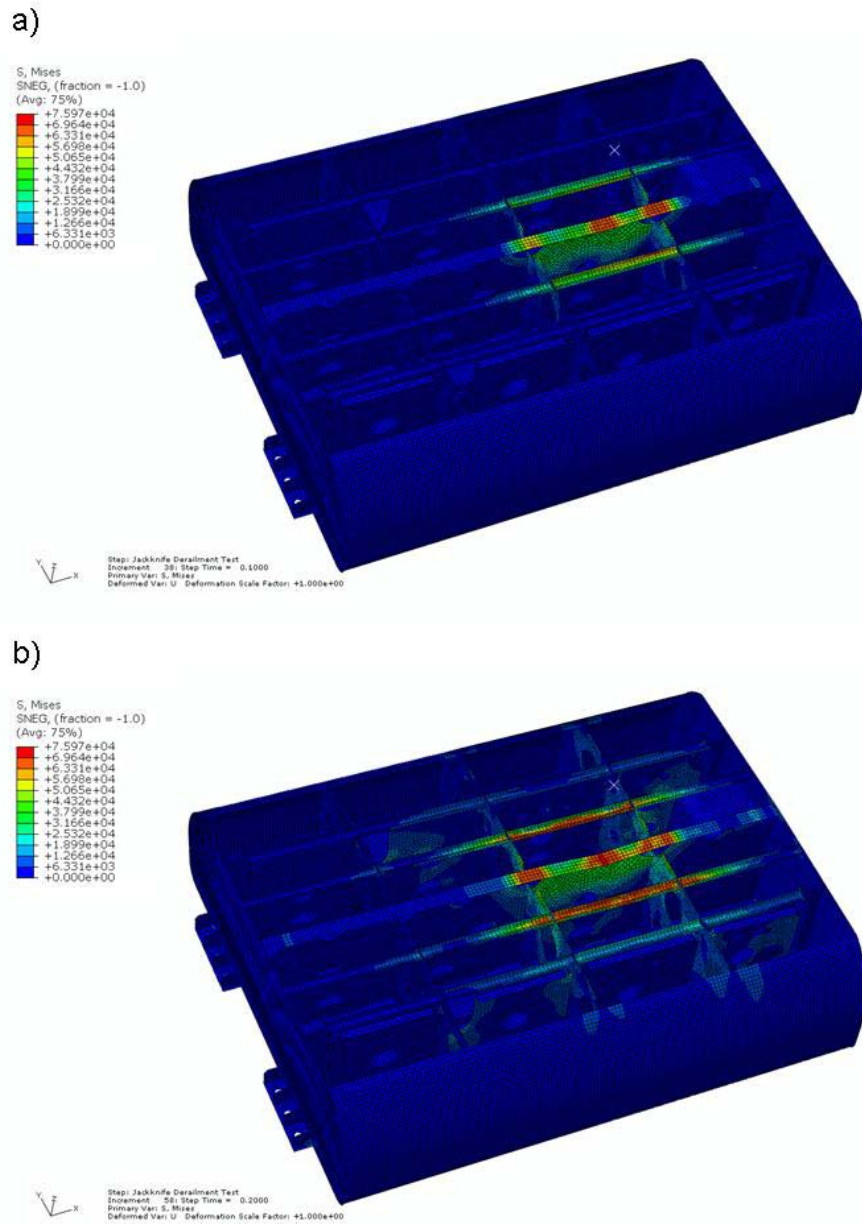


Figure 22. Comparison of Localized and Distributed von Mises Stresses in FEM: (a) just before 2.5-Inch Vertical Displacement and (b) after 2.5-Inch Displacement

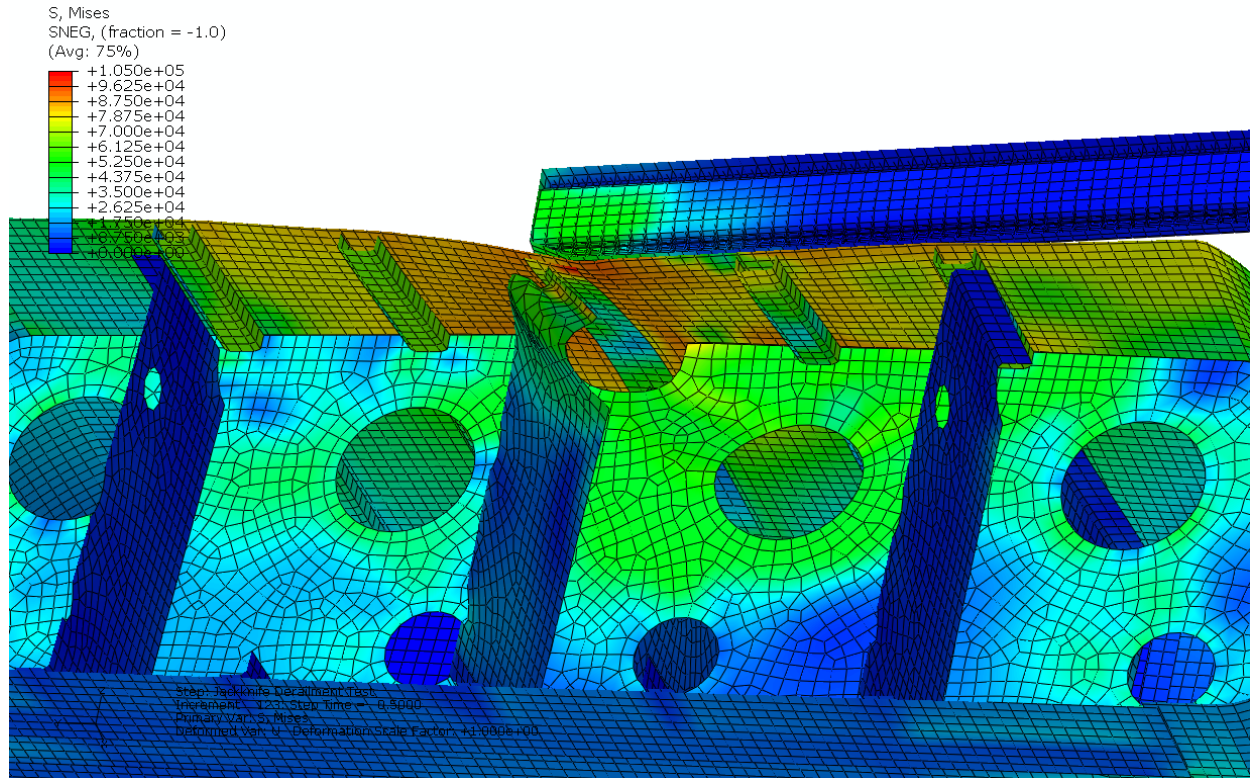


Figure 23. A Cutaway View of FEM Showing von Mises Stress Distribution in the Buckled Components under the Load Lever

5. Conclusions

The F59 PHI passenger locomotive fuel tank was subjected to simulated quasi-static JD load at FMI/QNA's fuel tank test facility. It was observed that the resulting vertical displacement of the bottom wall of the inverted tank corresponding to a maximum load of 317 kip was 4.1 in. This comprised both elastic and plastic displacements of the tank because of bending, as well as local vertical load-point displacement of tank bottom wall. Upon unloading, the local residual plastic deformation in the bottom wall was found to be approximately 1 in with no cracks or breach observed within the plastically deformed zone or elsewhere in the tank. The jackknife load versus vertical displacement behavior of the tank presented in Section 3 provides clear evidence of the tested tank's good load-bearing capacity. Hence, from the FRA regulatory perspective, the tank is deemed to have passed the structural integrity requirement and should be considered safe against JD loading.

Furthermore, a quasi-static implicit finite element code (ABAQUS) was used to model the F59 fuel tank. Comparison of the test and analytical simulation results showed good agreement up to the statutory JD load magnitude of 268 kip. Above this load, the FEM exhibited higher stiffness of the already deformed tank and therefore underpredicted the displacement. The simulation also provided insights into the nature of stress distribution and deformation behavior, especially in the internal components of tank.

6. References

National Instruments. (2008a). LabVIEW Version 8.2.1 with NI-Daq 4.3.

<http://www.ni.com/labview/>.

National Instruments. (2008b). Data Acquisition SCXI-1121/1120tb.

<http://sine.ni.com/nifn/cds/view/main/p/sn/n24:SCXI/lang/en/nid/1036/ap/daq>.

Requirements for External Fuel Tanks on Tier I Locomotives, Appendix D to Part 238, 49 CFR Ch. II (10-1-05 Edition), Federal Railroad Administration, U.S. Department of Transportation, 2005.

Appendix A. Summary of F59 Tank Material Tensile Properties Data

F59 Tank Materials Tensile Properties Data

1. Outer Longitudinal Baffle Plate

Nominal plate thickness =	0.1825 in
Coupon	F59-C1/2
Young's modulus, E =	28.7×10^6 psi
UTS =	69,432 psi
Elongation at UTS =	10.4 percent
Elongation at break =	22 percent
True stress at yield =	50,081.8 psi
True strain at yield =	0.001745

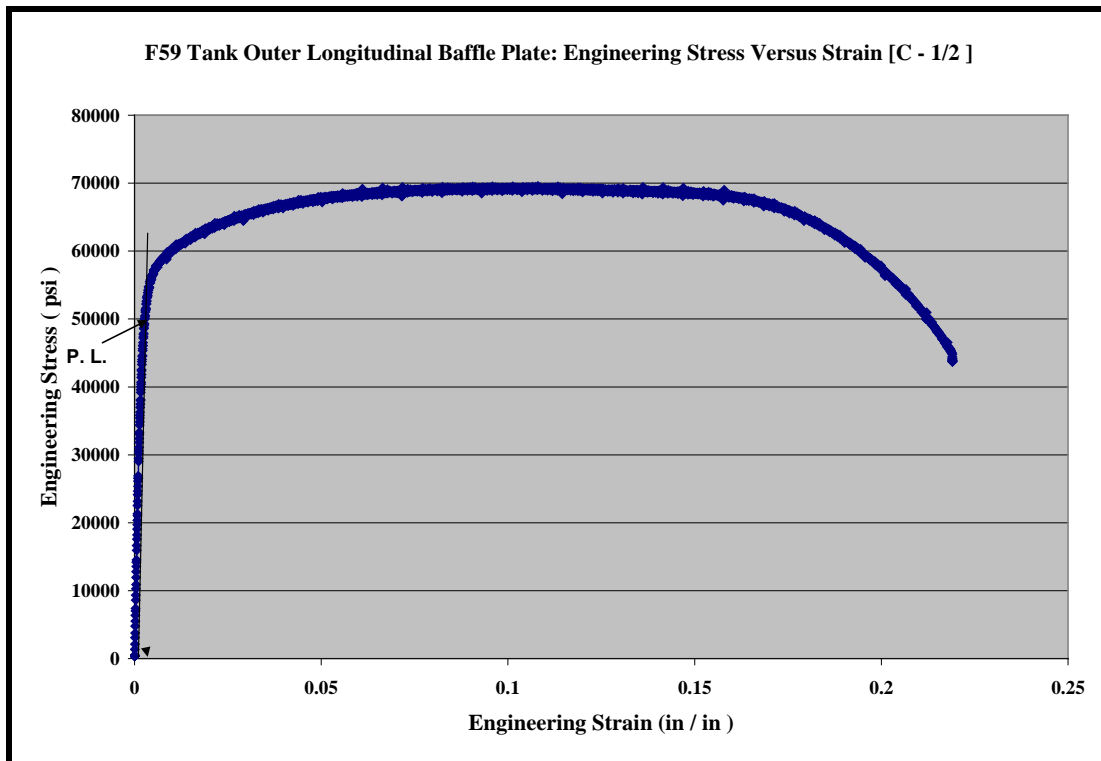


Figure A1. Engineering Stress vs. Strain Curve for Outer Longitudinal Baffle Plate

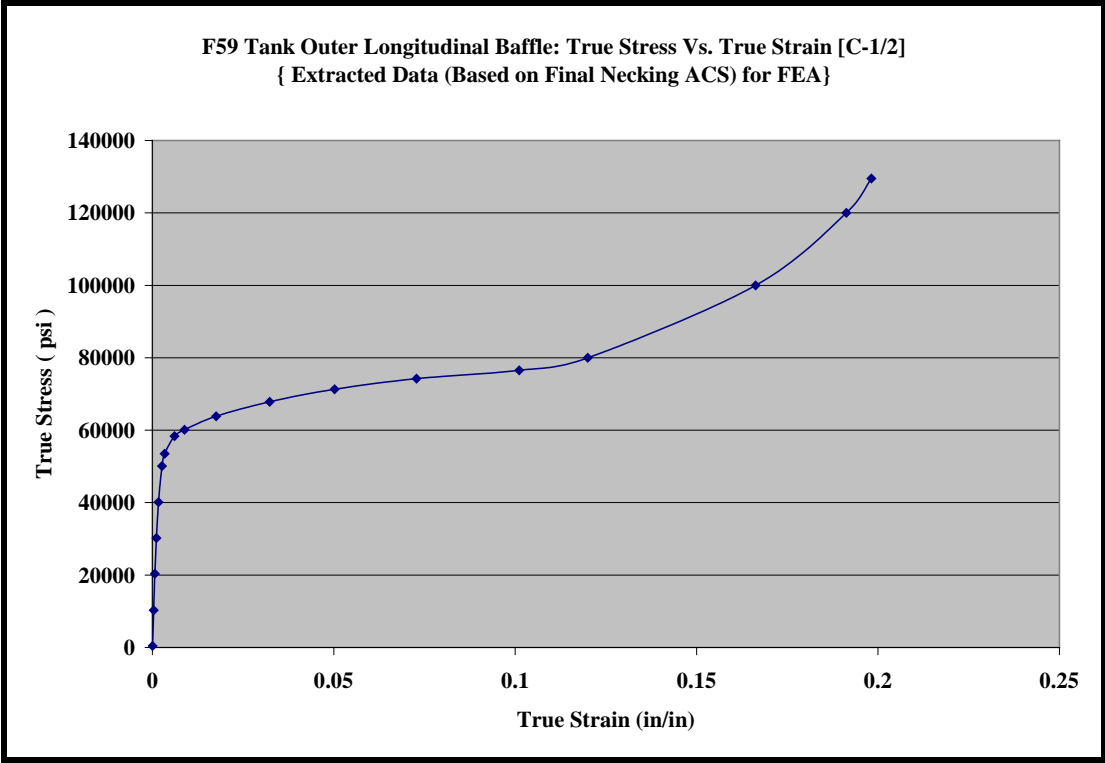


Figure A2. True Stress vs. True Strain Curve for Outer Longitudinal Baffle

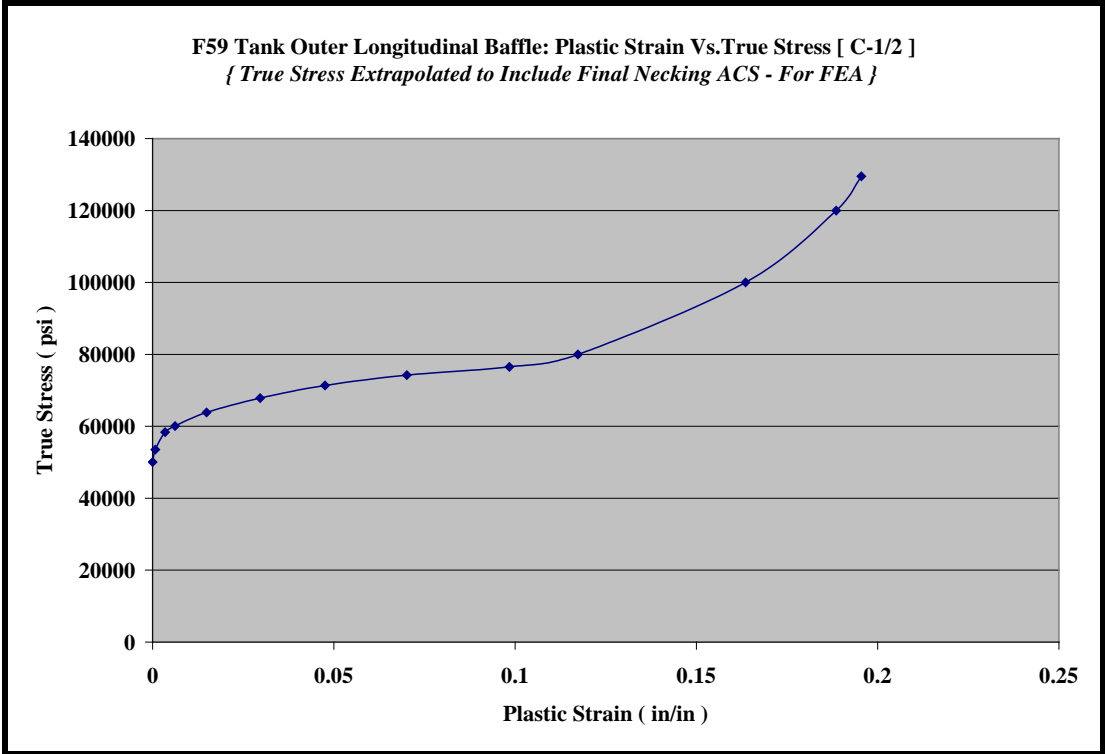


Figure A3. True Stress vs. Plastic Strain Curve for Outer Longitudinal Baffle

2. F59 Tank Central Longitudinal Baffle Plate

Nominal plate thickness =	0.2265 in
Coupon	F59-C2/1
Young's modulus, E =	13.0×10^6 psi (average value of two coupons tested)
UTS =	53,669 psi
Elongation at UTS =	16.75 percent
Elongation at break =	29.2 percent
True stress at yield =	31,014.8 psi
True strain at yield =	0.00238

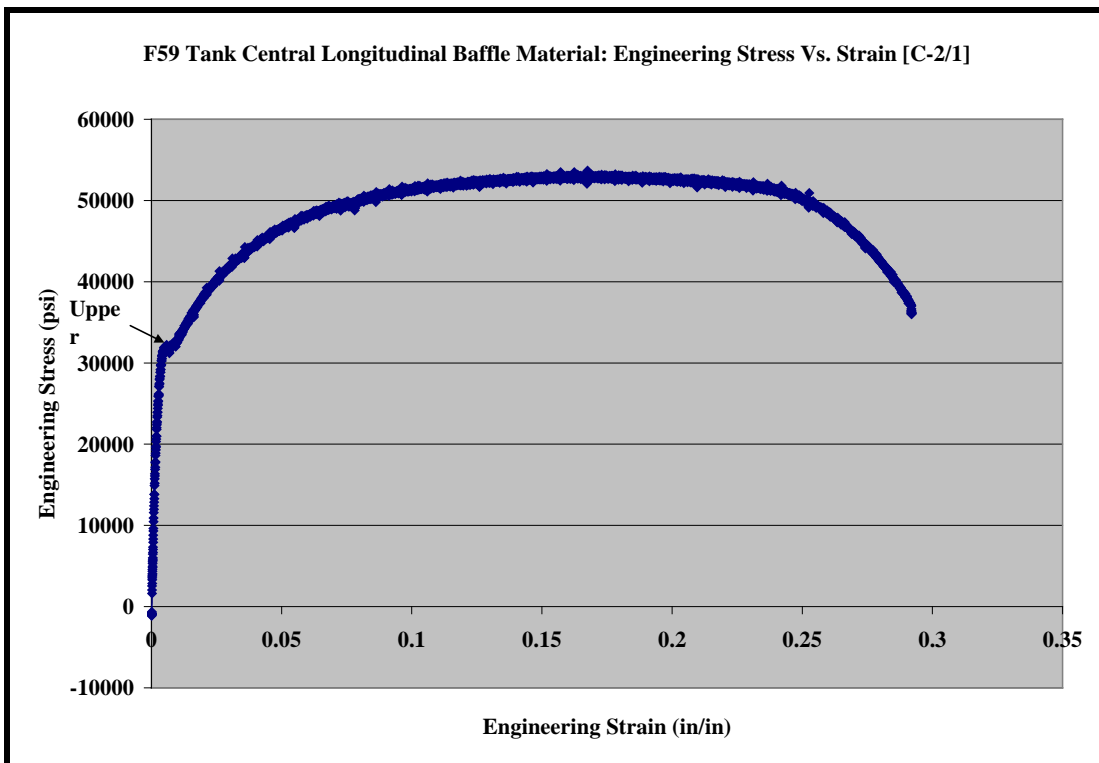


Figure A4. Engineering Stress vs. Strain Curve for Central Longitudinal Baffle Plate

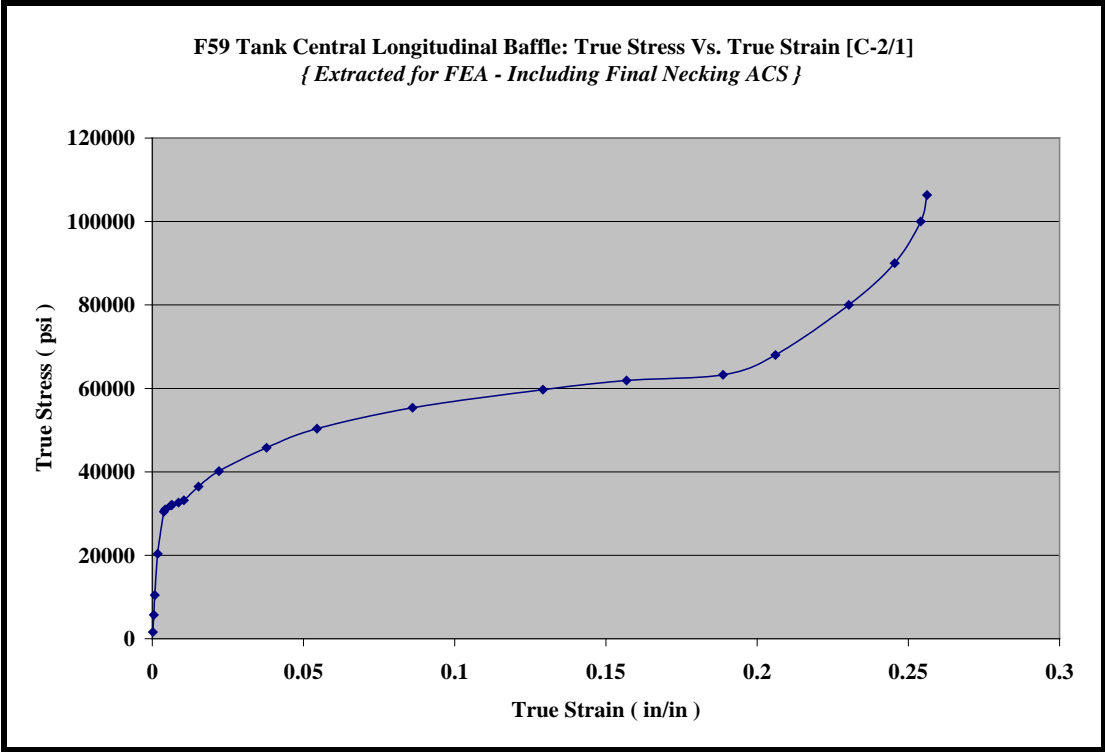


Figure A5. True Stress vs. True Strain Curve for Central Longitudinal Baffle

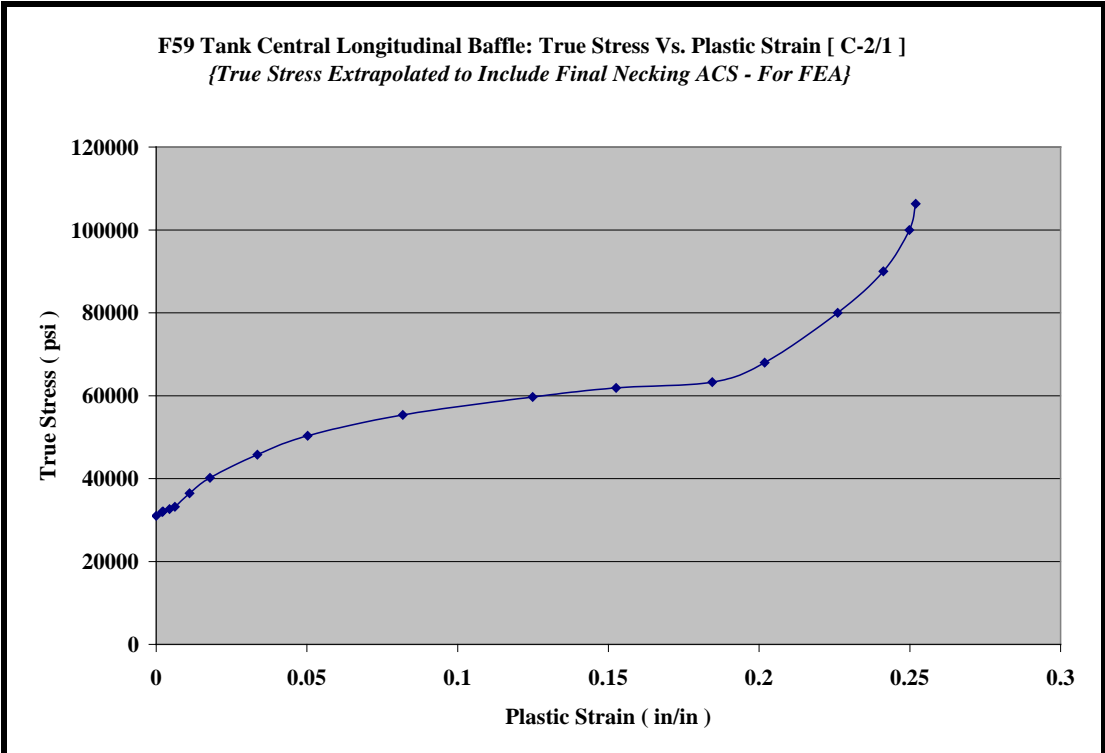


Figure A6. True Stress vs. Plastic Strain Curve for Central Longitudinal Baffle

3. F59 Tank Central Transverse Baffle Plate

Nominal plate thickness = 0.3705 in
Coupon F59-C3/1
Young's modulus, E = 29.513×10^6 psi
UTS = 69,475 psi
Elongation at UTS = 19.2 percent
Elongation at break = 37.9 percent
True stress at yield = 50,891.81 psi
True strain at yield = 0.001671

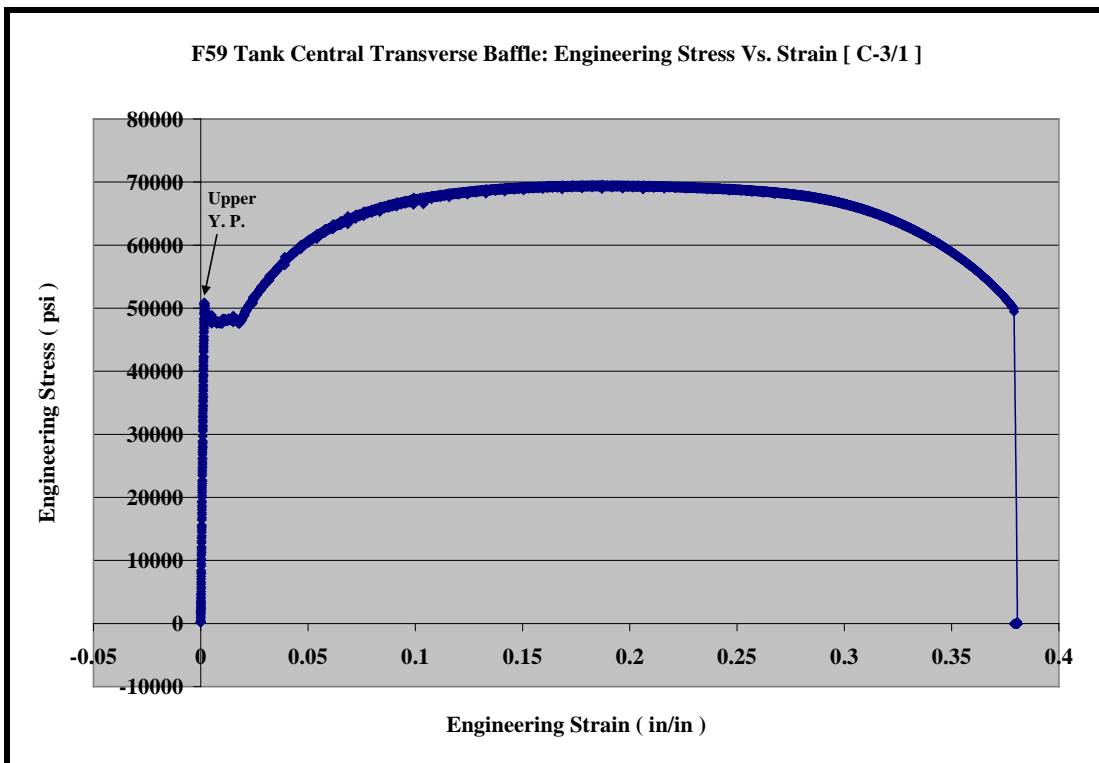


Figure A7. Engineering Stress vs. Strain Curve for Central Transverse Baffle Plate

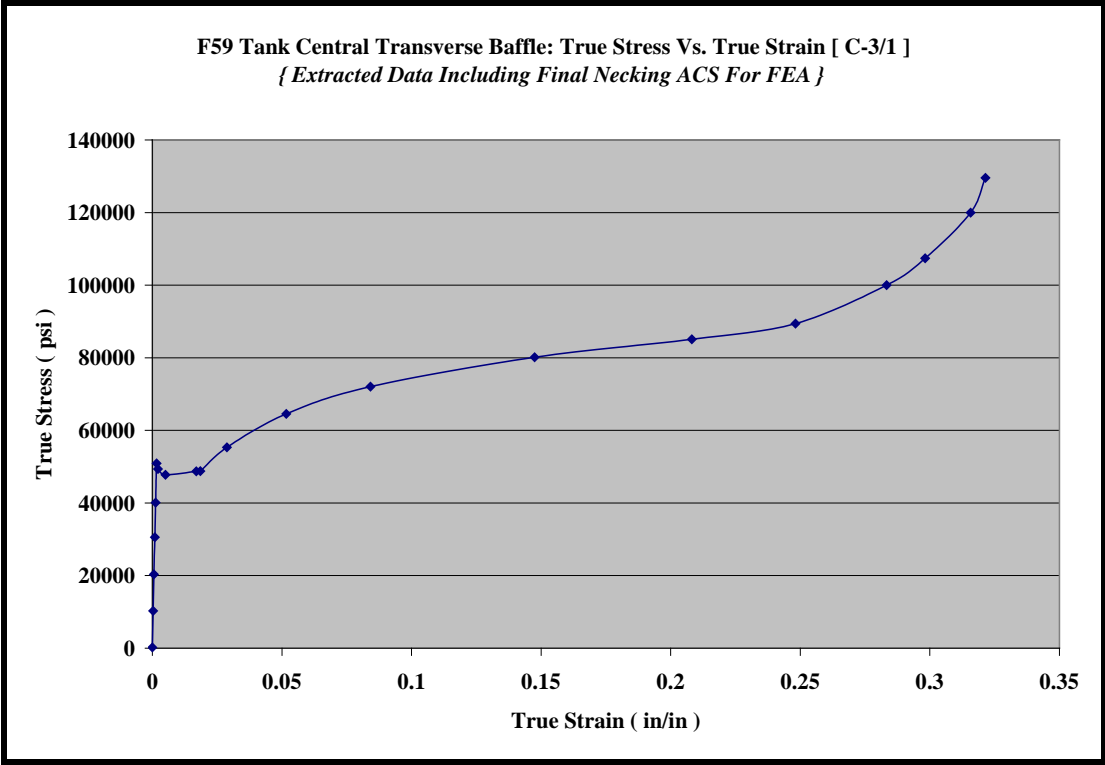


Figure A8. True Stress vs. True Strain Curve for Central Transverse Baffle

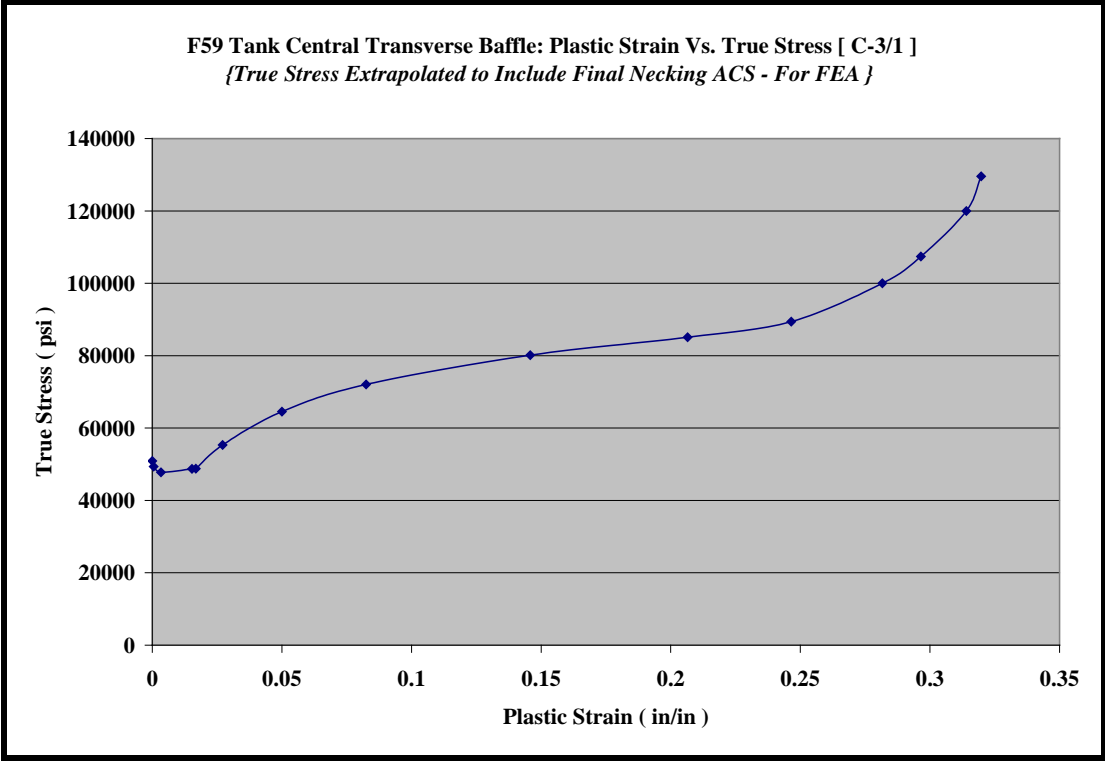


Figure A9. True Stress vs. Plastic Strain Curve for Central Transverse Baffle

4. F59 Tank Top Skin Plate

Nominal plate thickness = 0.25 in
Coupon F59-1-1
Young's modulus, E = 30.517×10^6 psi
UTS = 72,935 psi
Elongation at UTS = 14 percent
Elongation at break = 24.6 percent
True stress at yield = 65,834.65 psi
True strain at yield = 0.0023617

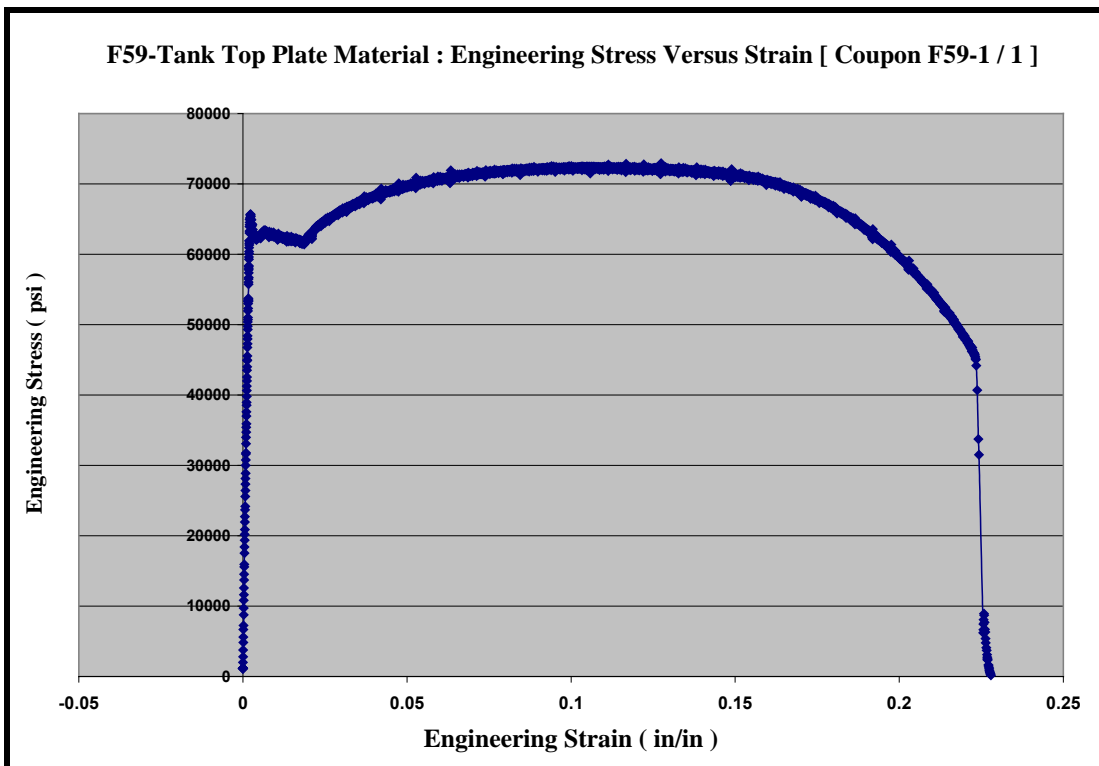


Figure A10. Engineering Stress vs. Strain Curve for F59 Tank Top Plate

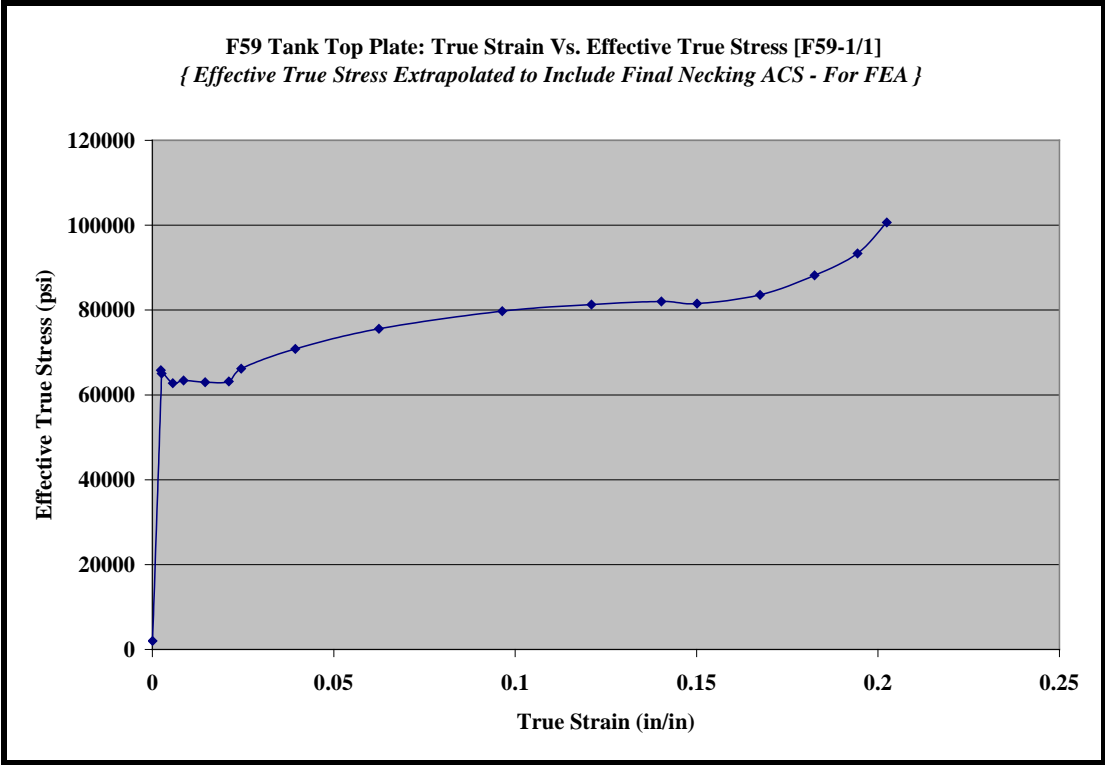


Figure A11. True Stress vs. True Strain Curve for F59 Tank Top Plate

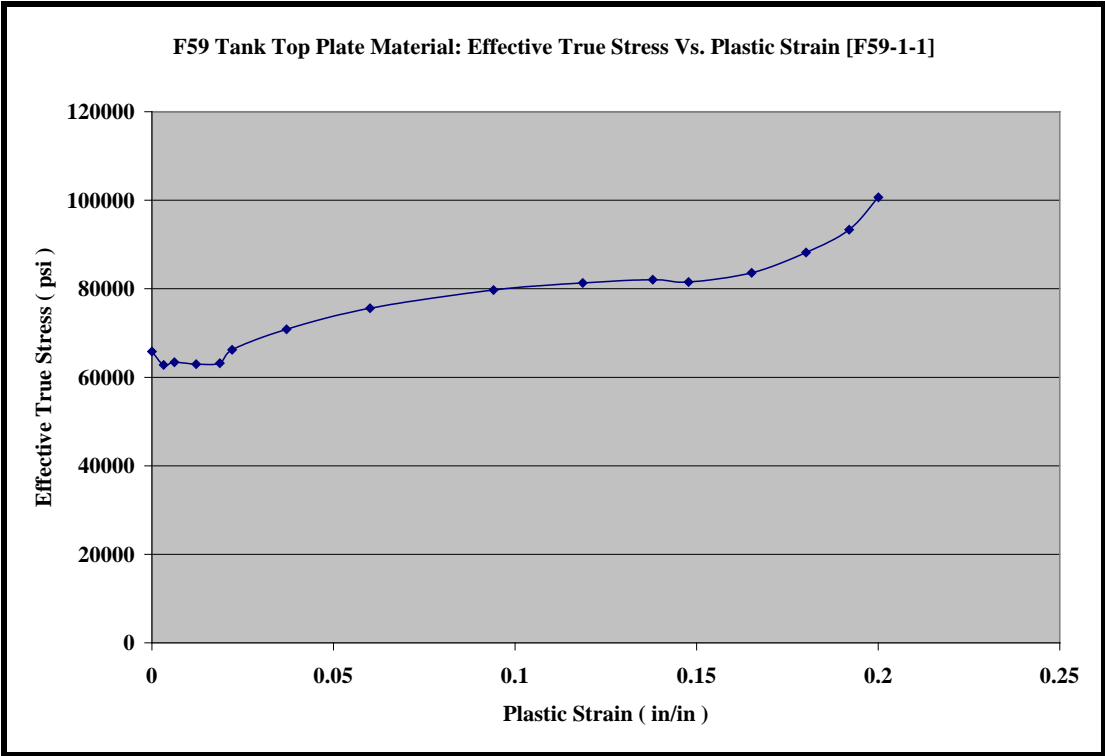


Figure A12. True Stress vs. Plastic Strain Curve for F59 Tank Top Plate

5. F59 Tank Bottom and Side Plate

Nominal plate thickness = 0.491 in
Coupon F59-4-2
Young's modulus, E = 29.422×10^6 psi
UTS = 88,662 psi
Elongation at UTS = 5.45 percent
Elongation at break = 25.1 percent
True stress at yield = 70,400 psi
True strain at yield = 0.002542

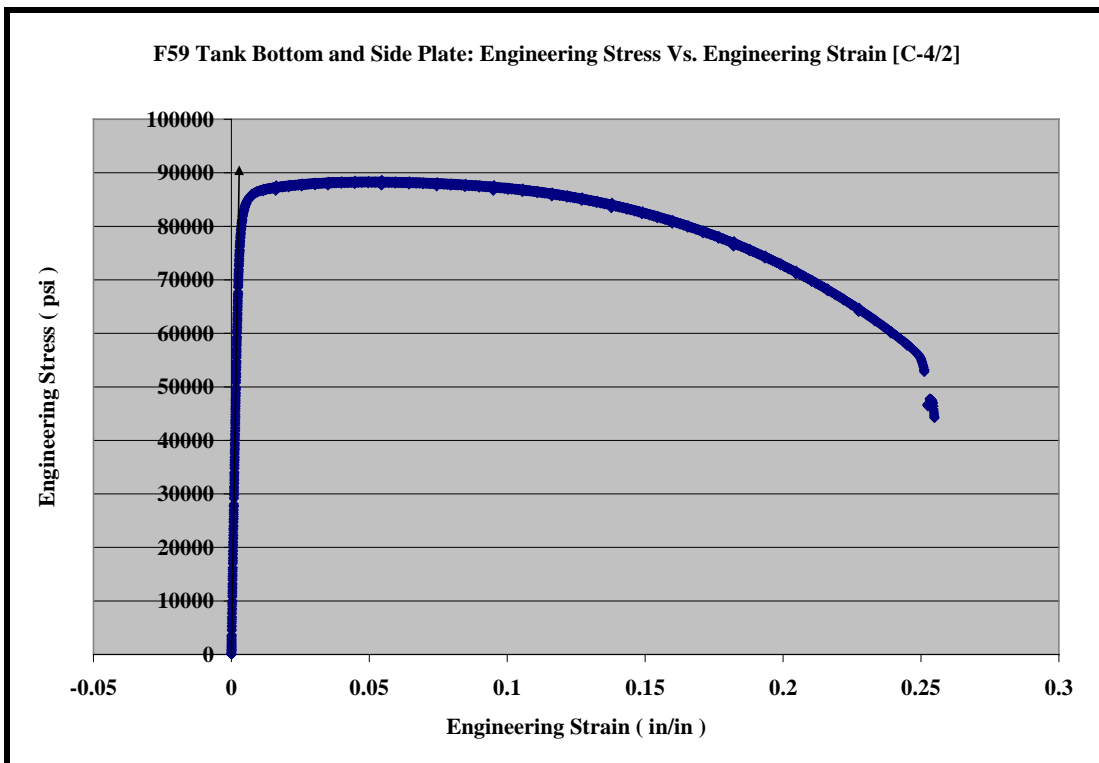


Figure A13. Engineering Stress vs. Strain Curve for F59 Tank Bottom and Side Plate

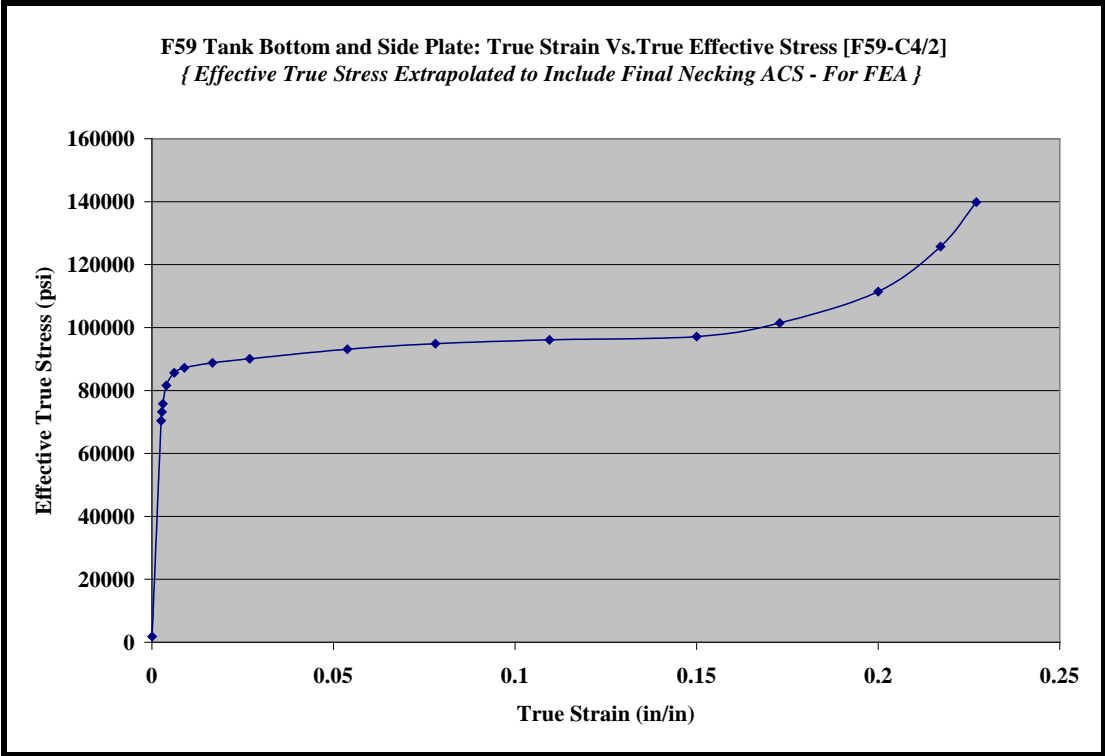


Figure A14. Effective True Stress vs. True Strain Curve for F59 Tank Bottom and Side Plate

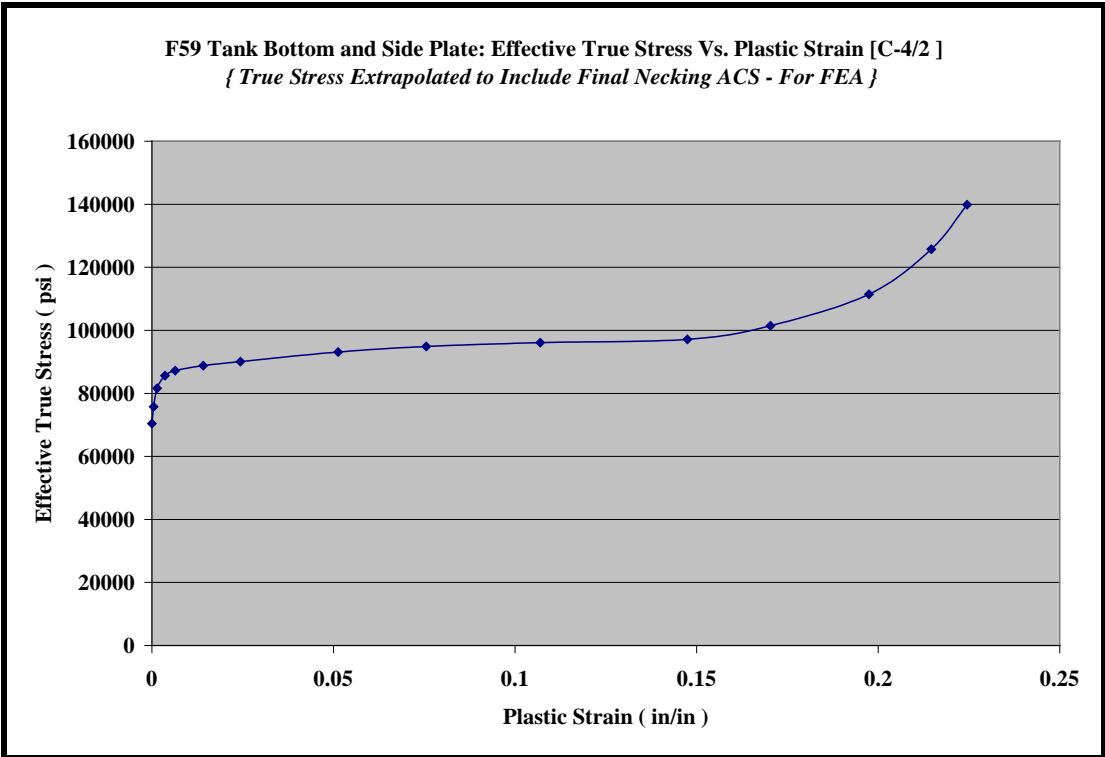


Figure A15. True Stress vs. Plastic Strain Curve for F59 Tank Bottom and Side Plate

6. F59 Tank End Plate

Assumed same material as SD70 tank

Nominal plate thickness =	0.75 in
Coupon	(SD70)-5/2
Young's modulus, E =	29.7×10^6 psi
UTS =	73,546 psi
Elongation at UTS =	11.34 percent
Elongation at break =	21.6 percent
True stress at yield =	51,581 psi
True strain at yield =	0.00171

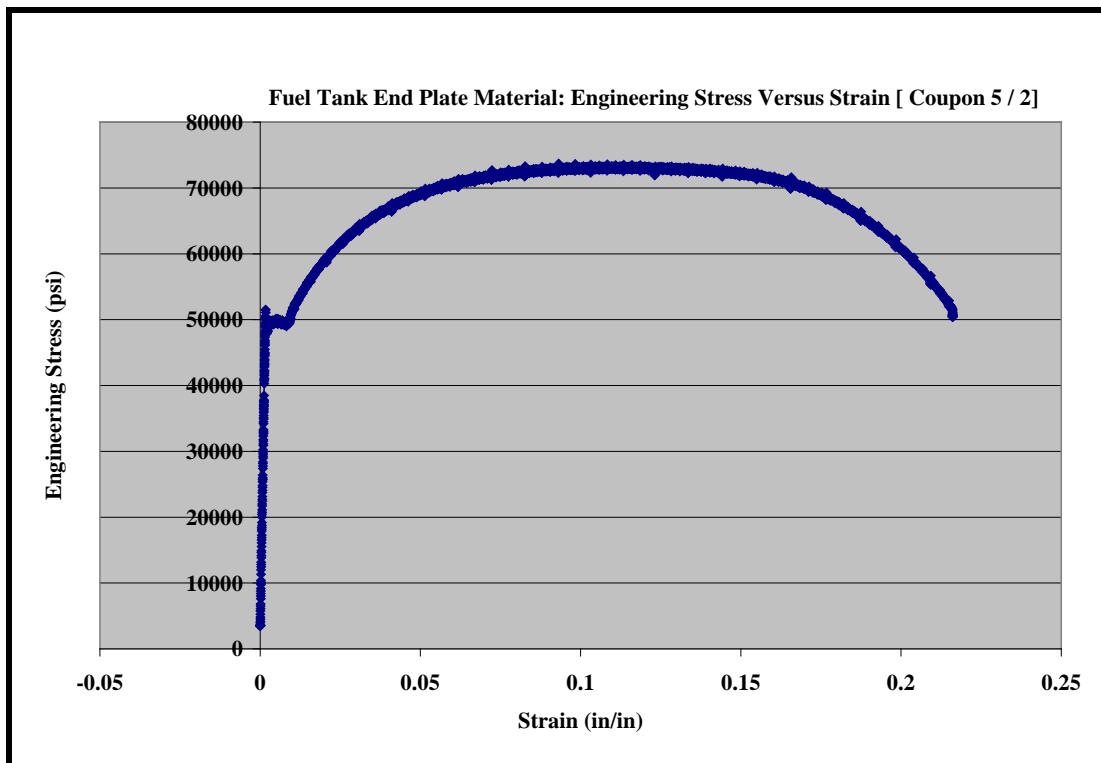


Figure A16. Engineering Stress vs. Strain Curve for Fuel Tank End Plate

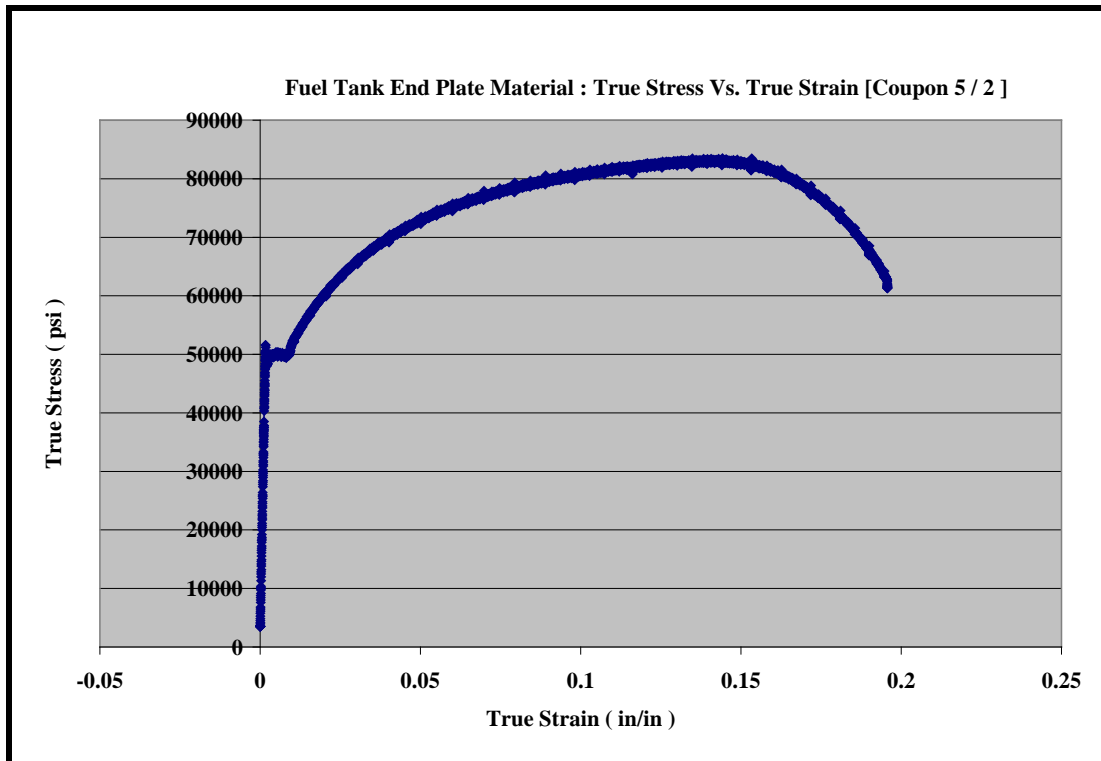


Figure A17. True Stress vs. True Strain Curve for Fuel Tank End Plate

Table A1. Summary of F59 Tank Materials Properties from Tensile Test Data

Component	Thickness (in)	Material	Modulus (Msi)	Yield Stress (ksi)	Ultimate (Msi)
Top plate	0.25	HSLA Steel	30.50	65.90	72.93
Bottom plate	0.491	CORTEN-B-QT70	29.40	70.40	88.66
Side plates	0.491	CORTEN-B-QT70	29.40	70.40	88.66
End plates	0.75	CORTEN-B	29.70	51.60	73.54
Transverse baffles	0.3705	AISI 1030/CORTEN-A	29.50	50.20	69.47
Longitudinal baffle (outer)	0.1825	CORTEN-A	28.70	50.10	69.43
Longitudinal baffle (center)	0.2265	Cast iron	13.00	31.90	53.70

Notes:

COR-TEN A refers to corrosion-resistant steel material of thickness less than 0.5 in.

COR-TEN B refers to same material with thickness in the range of 0.5–2.0 in.

QT70 represents thermomechanically processed (quenched and tempered) COR-TEN steel material to raise the yield stress from 50 to 70 ksi.

Abbreviations and Acronyms

AAR	American Association of Railroads
CAD	computer-aided design
CFR	Code of Federal Regulations
FEA	finite element analysis
FEM	finite element model
FRA	Federal Railroad Administration
HSLA	high-strength low-alloy
JD	jackknife derailment
kip	kilopound
ksi	kilopound per square inch
LabVIEW	Laboratory Virtual Instrumentation Engineering Workbench
lb	pound
MD	minor derailment
min	minute
Msi	million pounds per square inch
NI	National Instruments
psi	pound per square inch
SI	side impact